Biomaterials 33 (2012) 5230–5246

Contents lists available at SciVerse ScienceDirect

Biomaterials

journal homepage: www.elsevier.com/locate/biomaterials

Review

Engineering microscale topographies to control the cell–substrate interface

Mehdi Nikkhah [a,b,1,2], Faramarz Edalat [a,b,1,2], Sam Manoucheri [a,b,2], Ali Khademhosseini [a,b,c,*]

[a] Center for Biomedical Engineering, Department of Medicine, Brigham and Women's Hospital, Harvard Medical School, Boston, MA 02115, USA
[b] Harvard-MIT Division of Health Sciences and Technology, Massachusetts Institute of Technology, Cambridge, MA 02139, USA
[c] Wyss Institute for Biologically Inspired Engineering, Harvard University, Boston, MA 02115, USA

ARTICLE INFO

Article history:
Received 22 March 2012
Accepted 27 March 2012
Available online 21 April 2012

Keywords:
Surface topography
Microfabrication
Adhesion
Migration
Mechanobiology
Tissue engineering

ABSTRACT

Cells in their *in vivo* microenvironment constantly encounter and respond to a multitude of signals. While the role of biochemical signals has long been appreciated, the importance of biophysical signals has only recently been investigated. Biophysical cues are presented in different forms including topography and mechanical stiffness imparted by the extracellular matrix and adjoining cells. Microfabrication technologies have allowed for the generation of biomaterials with microscale topographies to study the effect of biophysical cues on cellular function at the cell–substrate interface. Topographies of different geometries and with varying microscale dimensions have been used to better understand cell adhesion, migration, and differentiation at the cellular and sub-cellular scales. Furthermore, quantification of cell-generated forces has been illustrated with micropillar topographies to shed light on the process of mechanotransduction. In this review, we highlight recent advances made in these areas and how they have been utilized for neural, cardiac, and musculoskeletal tissue engineering application.

1. Introduction

The microenvironment in which cells reside *in vivo* exhibits a complex milieu of signals which play an essential role in a diverse set of cellular processes [1]. Cells are capable of sensing and responding to a plethora of signals, consisting of biochemical and biophysical cues, over a wide range of length scales [2]. Many of these cues are provided by the extracellular matrix (ECM), which acts as a cellular scaffold and is the primary extracellular component of tissues [3]. *In vivo*, the ECM, through its structure and molecular composition, presents a variety of geometrically-defined, three-dimensional (3D) physical cues on the order of micron and sub-micron scale, known as topographies [4–6]. The ECM is composed of proteins and polysaccharides with structural widths and lengths in the nano- and micrometer range, respectively [7]. These individual ECM components are folded and bent to form secondary supramolecular structures—held by secondary and disulfide bonds, and hydrophobic interactions—with micron-size topographies [8]. The intestinal mucosa is a case in point illustrating the wide range of topographical length scales present *in vivo*. This tissue consists of finger-like projections known as villi which are epithelial folds 400–500 μm in dimension [9,10]. Each villi is further folded into smaller microvilli and at the base of each villi are epithelial invaginations known as intestinal crypts that are 100–200 μm in dimension. The intestinal mucosa is supported by a basement membrane containing surface pores 1–5 μm in diameter and 50 nm-thick collagen fibers. The interaction and response of cells with these topographies are mediated through a phenomenon called contact guidance [11]. Contact guidance is known to affect cellular behaviors such as adhesion, morphology, migration, and differentiation [12–16]. Another type of physical cue displayed by the ECM is mechanical stiffness through which, similar to topography, a diverse set of cellular functions can be modulated [17,18].

The effect of physical stimuli on cellular function has long been recognized [11,17–21]. Through a process known as mechanotransduction, various physical cues in a cell's surrounding environment are integrated and converted to biochemical, intracellular signaling responses that lead to changes in cell function [17,19]. At the nanometer length scale, the topography of the ECM affects sub-cellular behaviors such as the organization of the cell adhesion molecule receptors, whereas at the micron level, cellular and supracellular characteristics such as cell morphology and

* Corresponding author. Department of Medicine, Brigham and Women's Hospital, Harvard Medical School, PRB, Rm 252, 65 Landsdowne Street, Cambridge, MA 02139, USA. Tel.: +1 617 388 9271; fax: +1 617 768 8202.
E-mail address: alik@rics.bwh.harvard.edu (A. Khademhosseini).
[1] M.N. and F.E. contributed equality to this work.
[2] Post address for co-authors: Partners Research Building, Room 252, 65 Landsdowne Street, Cambridge, MA 02139, USA.

0142-9612/$ – see front matter © 2012 Elsevier Ltd. All rights reserved.
doi:10.1016/j.biomaterials.2012.03.079

migration, and tissue organization are influenced. Hence, the ECM conveys biophysical signals over a broad range of length scales from nano- to micrometers [18]. Despite the significance of these processes, the underlying mechanism of how physical stimuli contribute to the regulation of cellular behaviors has yet to be fully understood.

By understanding the manner in which cells interact with their physical environment, it may be possible to control cellular behavior through the fabrication of substrates with unique physical properties. In pursuit of understanding these interactions, nano- and microfabrication technologies are being widely used to construct substrates of differing topographies. In this regard, nanotechnology has been used to create sub-100 nm topographical features to investigate the supramolecular events occurring at the cell–substrate junction [22]. In contrast, microfabrication techniques have gained notoriety for their ability to affect supracellular behavior and to develop inexpensive, scalable features with high precision and fidelity [23]. Therefore, many biologists and bioengineers have added microfabrication techniques, used to generate microtopographies, to their armamentarium to study specific cell behaviors [24–28]. The capability of microfabrication techniques in generating various topographical stimuli mimicking native cell microenvironment's architecture has provided valuable insight to scientists about the relationship between the cell–substrate interaction and cellular processes such as adhesion, migration, and differentiation across different tissues (Fig. 1) [1,29]. In addition, these techniques have allowed for the design of platforms invaluable to studying cell biomechanics at the micrometer length scales and its importance in tissue organization and development.

In this review, recent developments toward understanding the effect of topographical cues on cellular behaviors are highlighted. Of particular interest in this review are microscale topographies with dimensions that are greater than 1 μm. Various microfabrication technologies used to develop topographical features for the study of cell–substrate interactions are discussed. Specifically, we will focus on the effect of these interactions on cell adhesion, morphology, migration, and differentiation (Table 1). Consequently, the application of microscale topographies to study cellular forces and mechanics is reviewed. Furthermore, we will highlight the use of these topographies in constructing substrates for nerve, cardiac, and musculoskeletal tissue engineering applications. Finally, future directions and challenges in using topography to gain a deeper understanding of cellular processes are discussed.

2. Fabrication techniques

Various fabrication techniques are used to produce ordered or randomly structured microtopographies. Randomly structured microtopographies can be generated with classical processing methods such as sandblasting and grit-blasting [30–33], polishing, grinding [34], abrasion [35], plasma spraying, acid etching, and machining [36,37]. In contrast, microfabrication can produce surfaces with ordered structures such as grooves, pillars, pits, and wells. The foundations of microfabrication techniques arose from the semiconductor and microelectronics industries where it was initially used to fabricate integrated circuits of microprocessors at micrometer length scales. In biology, many of the components of a cell's environment are on the order of nano- to micrometer scale. For instance, the width of a single collagen fiber is 0.5–3 μm and the length of cells range from 1 to 100 μm. Thus, it has become clear that a greater degree of control over a cell's behavior is needed at these length scales. Over the past two decades, microfabrication technologies have been instrumental in enabling more precise manipulation of cells and hence, have come to be increasingly applied to biology, medicine, and biomedical engineering [38]. The introduction of microfabrication to biological experiments has

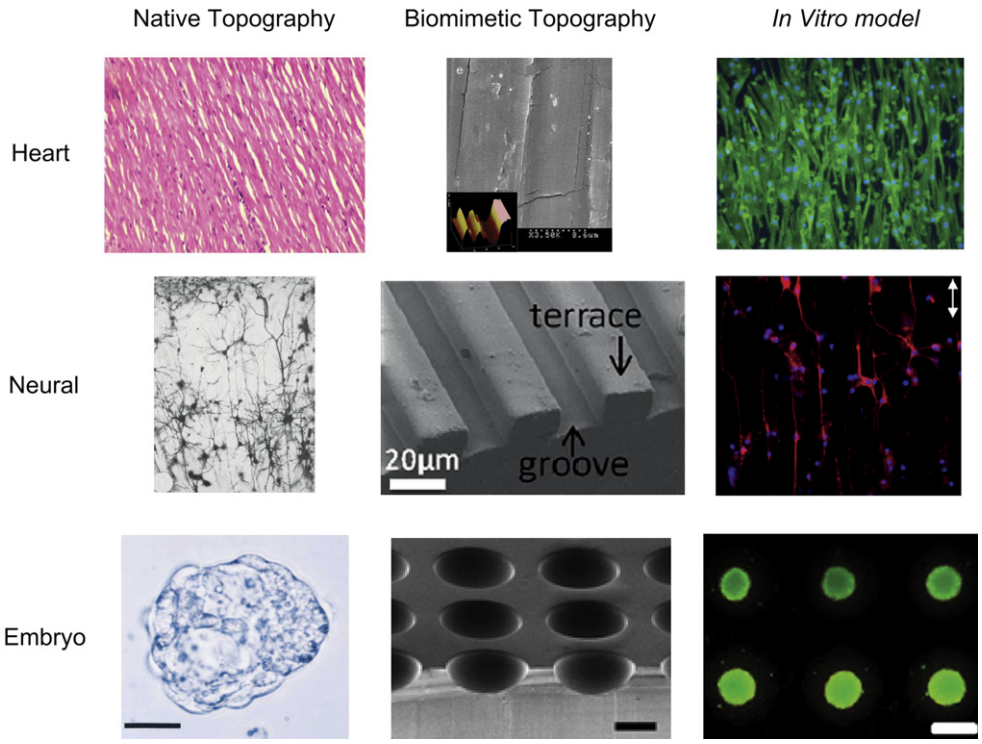

Fig. 1. Mimicking *in vivo* embryo, neural, and cardiac tissue organizations via fabricated microtopographies in *in vitro* platforms [35,141,229–232]. Scale bars, 20 μm (bottom left), 500 μm (bottom middle, bottom right). Adapted with permission from BioMed Central: [BMC Pharmacology]. Adapted with permission from Elsevier: [Biomaterials], copyright (2007), [Brain Research], copyright (1968), [Biomaterials], copyright (2012), [Cell], copyright (1996), [Biomaterials], copyright (2010).

Table 1
Summary of selected studies on the effects of microscale topographies on cell adhesion and morphology.

Substrate type	Cell type	Substrate material	Feature size	Significant findings
Grooves	Embryonic *Xenopus* spinal cord neurons, rat hippocampal neurons	Quartz	1, 2, 4 μm width 14 nm–1.1 μm depth	*Xenopus* cell alignment along the grooves of all sizes; hippocampal cell alignment along wide and deep grooves [76].
	Human gingival fibroblasts	Ti-coated silicon	15 μm width 3 μm depth	Primary elongation of microtubules along the grooves followed by elongation of actin fibers and focal contacts [78].
	Human gingival fibroblasts	Ti-coated silicon	0.5–15 μm width 0.5, 3 μm depth	Alignment of microtubules and actin fibers along the grooves [79].
	Human osteoblasts	Ti- and HA-coated silicon	4–38 μm width 2, 4, 10 μm depth	Improved alignment on feature dimensions close to the cell size. Similar contact guidance on Ti and HA substrates [80].
	Primary human foreskin fibroblasts, keratinocytes	Ti-coated silicon, Ti-coated epoxy resin (Araldite®)	1–20 μm width 0.4–2 μm depth	Fibroblasts were oriented while keratinocytes failed to orient along the grooves. Adhesion of cells to the substrate could be improved through coating the surface with Ti [81].
	Osteoblasts, myoblasts	HA-coated silicon	8, 24 μm width 2–10 μm depth	Better alignment of myoblasts compared to osteoblasts on groove features. Enhanced alignment on microgrooves were cell specific [82].
	Transfected human corneal epithelial cells	Silicon	0.2–2 μm width 0.4 μm depth	Elongation and cytoskeletal orientation along the grooves [77].
	BHK, MDCK, chick embryo cerebral neurons	PMMA	2–12 μm width 0.2–1.9 μm depth	Alignment of all cell types enhanced with decreasing groove width and increasing groove depth [83].
	Rat dermal fibroblasts	PS	1–20 μm width 0.5–5.4 μm depth	Orientation of the cells enhanced with increasing groove depth [85].
	Rat dermal fibroblasts	PS, PLA, Ti, Silicone	1–10 μm width 0.5 μm depth	Best alignment on 1 μm-wide PLL grooves. Cells morphology changes based on the type of material used [84].
	Rat PC-12 cells, chick sympathetic neurons	PLA	1, 2 μm width 150–215 nm depth	Guided neurite alignment and extension on grooved features [86].
	Rat dermal fibroblasts	PDMS	2, 5, 10 μm width 0.5 μm depth	Enhanced alignment of cells on 2 and 5 μm grooves. Similar behavior on 10 μm grooves as to those on flat surfaces [92].
	Rat dermal fibroblasts	PDMS	2, 5, 10 μm width 0.5 μm depth	Enhanced orientation of actin fibers and vinculin along 2 μm-wide grooves compared to 5 and 10 μm grooves [93].
	Endothelial cells	PDMS	3.5 μm width 0.2–5 μm depth	Enhanced alignment of cells with increasing groove depth. Alignment of F-actin and vinculin along the grooves [90].
	Human endothelial, fibroblast and smooth muscle cells	PDMS	2–10 μm width 0.05–0.2 μm depth	Enhanced alignment of all cell types with decreasing groove width and increasing groove depth [91].
	C2C12 myoblasts	Poly-carbonate	5–75 μm width 5 μm depth	Enhanced cellular nuclear alignment along 10 μm groove features [87].
	Bovine aortic endothelial cells	PGS	2–5 μm width 0.45 μm depth	Enhanced cellular alignment along 2 μm-wide patterns compared to 5 and 10 μm-wide grooves, and flat surfaces [88].
	Endothelial cells	Olefin copolymer	1, 5 μm width 0.1–2 μm depth	Enhanced alignment and polarization of cells on 1 μm-width and 1 and 5 μm depth grooves compared to flat surfaces [89].
Pillars, posts	LRM55 astroglial cells	Silicon	0.5–2 μm diameter 1 μm depth	Majority of cells showed preferential adhesion to the top of the pillars. Highly polarized cytoskeleton on pillars [95].
	NIH-3T3 fibroblasts	PS	10 μm diameter 2 μm depth	Branched morphology and stable FAs for cells that were cultured on pillars [96].
	NIH-3T3 fibroblasts	PDMS	5–10 μm diameter 2–10 μm depth	Branched morphology of cells attached to the top of the pillars. Similar morphology on shorter pillar compared to 2D surfaces. Bi- to tripolar morphology on pillars widely spaced apart [97].
	NIH-3T3 fibroblasts, HeLa, primary hepatocytes	PDMS	1.25–9 μm diameter 2.5 μm depth	Better attachment of cells on pillars with smaller diameter independent of the cell type [98].

Table 1 (*continued*)

Substrate type	Cell type	Substrate material	Feature size	Significant findings
	Human skin fibroblasts	Tantalum-coated silicon	1–6 μm diameter 2.4 μm depth	Stellate-like cell shape along with diffuse cytoskeleton for large inter-pillar gap sizes [99].
Pits	OCT-1 osteoblast-like cells	PLA, PS	0.45, 2.2 μm diameter	Cell stretched on convex islands while they crossed over pits with small diameters. Pseudopods were shown to intrude inside the pits. The attachment efficiency was higher on topographies compared to 2D surfaces [101].
	Rat calvarial osteoblasts (RCO), Porcine periodontal ligament epithelial cells (PLE)	Ti-coated epoxy	45, 175, 270 μm width 30, 120 μm depth	PLE cells exhibited increased spreading with mature FAs whereas RCO cells formed smaller adhesions on tapered pits [102].
Pyramids	Endothelial cells	RGD-coated Silicon	0.05–1.8 μm height	Fewer number of cells attached on surfaces with pyramidal topographies compared to 2D surfaces. RGD concentration was a major factor affecting cell spreading [103].
Isotropically-etched cavities	HS68 human fibroblasts, MCF10A normal human breast epithelial, MDA-MB-231 metastatic breast cancer cells	Silicon	150–170 μm diameter 50–70 μm depth	Fibroblast cells stretched while MDA-MB-231 and MCF10A cells adopted a shape similar to the curved surfaces of the isotropic microstructures [105,106].
	MCF10A normal human breast epithelial, MDA-MB-231 metastatic breast cancer cells	Silicon	140–170 μm diameter 50–70 μm depth	Treatment of the MDA-MB-231 cells with anti-cancer drugs significantly altered morphology, adhesion, and cytoskeletal organization of cells within the etched cavities [107,108].

BHK: Baby hamster kidney fibriblasts, HA: hydroxyapatite, MDCK: Madin–Darby Canine Kidney, PDMS: poly(dimethylsiloxane), PGS: poly(glycerol-sebacate), PLA: poly-L-lactic, PMMA: poly(methyl methacrylate), PS: polystyrene, Ti: titanium, Rat PC-12 : Rat adrenal pheochromocytoma cell line.

made it possible to control the cellular microenvironment through modulating cell–cell and cell–substrate interactions, and create high-throughput systems to carry out parallel experiments [23].

Photolithography, a method in which light is used to generate structures on a surface, was among the first fabrication methods applied to the field of biology. This technique is widely used to generate rigid microstructures on inorganic materials such as silicon and silicon oxide [39,40]. In this technique, the substrate is spin-coated with a layer of light-sensitive polymer called photoresist (*e.g.* SU-8). The photoresist layer is selectively exposed to ultraviolet light through a mask layout that causes crosslinking, polymerization, or degradation of the exposed material. The pattern is then developed through various means which results in dissolution of selected areas. Using photolithography, two-dimensional (2D) or topography-containing substrates, as well as cell-encapsulated materials may be constructed with many different natural and synthetic polymers [41–43]. Due to light diffraction, the resolution of the irradiated patterns is approximately on the order of the wavelength of light used [39,40,44]. Therefore, smaller features can be generated through using particles with shorter wavelengths such as x-rays and electron beams (electron beam lithography). Photolithographic techniques have been widely used to create topographies such as grooves and wells for cell adhesion and migration analysis [45,46].

After photolithographic patterning, the areas of the substrate which are not covered by the photoresist layer can be etched isotropically or anisotropically using wet or dry chemical etching processes. Depending on the type of etchant and crystal orientation of silicon substrate, wet chemical etching usually results in isotropic features with curved surfaces or anisotropic features with v-shaped cross sections. On the other hand, dry etching processes, such as deep reactive ion etching (DRIE) and reactive ion etching (RIE) are mainly used to develop anisotropic microstructures with square cross sections and vertical sidewalls [47,48]. Recent reports have shown that it is possible to generate isotropic microstructures comprised of curved surfaces by varying the geometrical patterns of the mask layout and using DRIE. This fabrication approach, which is used to etch silicon to different depths using a single-etch step process, is based on the applicability of RIE lag and its dependence on the geometrical patterns of the mask layout [49,50].

Stereolithography and two-photon absorption lithography [51] are mask-less fabrication methods for creating 3D structures, particularly with desired topographies for tissue engineering applications [52,53]. In stereolithography, UV laser is used to polymerize photosensitive monomeric or polymeric resins within predefined regions. Hence, in this technique, a 2D pattern can be obtained, although 3D patterns are possible through a layer-by-layer approach [54]. In contrast, in two-photon absorption lithography, an ultrafast laser is focused on photocurable resins to produce 3D structures. The fabrication of a 3D structure is controlled by the movement of the focus via piezo stages or galvo-scanners [55]. While stereolithography and two-photon absorption lithography have not been extensively used to generate topographies for biological studies, thus far it has been used to create nerve guidance conduits [56], and it is expected to be more prominent in the future given its high degree of control over constructing 3D microenvironments for tissue engineering applications.

Soft lithography refers to a set of techniques, which use elastomeric polymers to develop patterns based on embossing, molding, and printing methods [57]. The major advantages of soft lithography techniques are their low cost, ease of use, high-throughput nature, and high accessibility to biologists, chemists, and materials scientists without the need for expensive clean room facilities. An original master is usually fabricated via photolithography or silicon etching. Subsequently, the master is used to emboss structures onto an elastomeric material. The patterned elastomer can then be used to create topographies via replica molding, micromolding in capillaries, microtransfer molding, and microfluidics [57–59]. Numerous studies have used replica molding to develop 3D topographies through casting or embossing polymeric replicas on the original master or elastomeric molds [60]. Both rigid and elastomeric molds may be used to replicate the polymeric materials [61]. Poly(dimethylsiloxane) (PDMS) is the most widely used material in soft lithography given its biocompatibility, permeability to oxygen and carbon dioxide, and transparency for

optical imaging [62]. Soft lithography provides an approach to make features over large surface areas and with curved shapes, and overcomes the diffraction limitations of photolithography. This technique is typically used to fabricate micron-sized patterns. Its resolution can be less than 1 μm, limited primarily by loss of the mechanical integrity of the elastomer at smaller length scales [63]. In the biological sciences, soft lithography has been utilized to make various topographies to modulate cell behavior and study mechanobiology [28].

3. Cell adhesion and morphology

The majority of cells in the body are anchorage-dependent and necessitate adherence to the ECM or other cells to survive and function in a physiological manner [64]. Lack of adherence of these cells to substrates results in apoptosis, termed anoikis, and is an important consideration in cell transplantation therapies. *In vitro*, prior to cell attachment, an interfacial layer of proteins or biomolecules from the cell culture media (*e.g.* serum components) is formed from their adsorption onto the substrate's surface that subsequently influences cell attachment. A number of cellular structures are involved in the probing and sensing of the microenvironment and dictate cell attachment and morphogenesis. These include integrins in cell-ECM contact [65], cadherins in cell–cell adhesion [66], stretch-sensitive ion channels [67], Tyr kinase receptors [68], and G protein-coupled receptors [18]. In the cell-ECM interplay, integrins are part of a larger supramolecular complex, known as focal adhesion (FA), that link the ECM to intracellular components. The integrin-mediated mechanotransduction occurs through a series of intracellular molecular pathways and amplifications that lead to cytoskeletal changes [17,20]. For instance, increased local tension results in the clustering of integrins and phosphorylation of FA kinases [69], followed by activation of small GTPases of the Rho-family, such as RhoA. RhoA and its effector RhoA kinase (ROCK) are known to be involved in actin remodeling and modulation of transcription factors and gene expression [20,70]. Integrins also transmit ECM signals more directly through its physical connection with the actin filaments of the cell [71,72]. Substrate topography, imparted by ECM or microfabricated substrates, influences the organization, arrangement, and distribution of integrins. Upon integrin engagement with the underlying substrate, through a series of intracellular signaling cascades involving FA complexes and cytoskeletal filaments, cells start to spread and sense the topographical features of the underlying substrate [73,74]. This ultimately alters the cytoskeletal organization and force balance, which in turn changes cell morphology and cell function [75].

To date, a large body of the literature has focused on the role of microscale topographies in regulating cell adhesion and morphology. Microscale grooves are among the most common fabricated topographical features that have been employed to control these aspects of cell behavior. The materials used to fabricate grooved topographical features to investigate cell–substrate interactions include quartz [76], silicon [77], titanium-coated silicon [78–81], hydroxyapatite (HA)-coated silicon [82], poly(methyl methacrylate) (PMMA) [83], poly-L-lactic (PLA), polystyrene (PS) [84–86], polycarbonate [87], poly(glycerol-sebacate) (PGS) [88], olefin copolymers [89], and silicone/PDMS [90,91]. Grooved features are typically arranged in repeating patterns with equal groove and ridge widths and set groove depth. The majority of cell types cultured on these topographies align along the major axis of grooves, with their alignment and orientation enhanced on decreasing groove width and increasing groove depth [76–93]. Coupled with an elongated morphology, cytoskeletal elements such as actin fibers and microtubules display a directional organization parallel to the grooves' long axis [77–79,90,93]. In addition, alignment and localization of the FA complexes has been shown to be directly correlated with the cytoskeletal organization of cell [94]. For instance, early studies by Oakley and Brunette showed the alignment and cytoskeletal organization of human gingival fibroblasts on 1–30 μm-wide grooved titanium substrates [78,79]. In these studies, it was confirmed that microtubules were the first cytoskeletal component to orient along the direction of grooves, followed by actin fibers. In another work, Langer and colleagues developed parallel grooved-topographies with rounded edges on PGS substrates using replica molding to address contact guidance of bovine aortic endothelial cells for potential tissue engineering applications (Fig. 2a,b) [88]. The wavelength of the features was varied between 2 and 5 μm, while the depth was 0.45 μm. Their finding demonstrated that cells on microstructures with a smaller pitch size exhibited spindle-like morphology, a higher frequency of alignment, and a greater cell shape index compared to flat surfaces. In a recent study, nanoimprint lithography was used to fabricate grooved features in olefin copolymers to study endothelial cell organization and alignment for potential application in designing implantable biomaterials. The ridge width was selected to be 1 or 5 μm, while the groove depth was varied from 0.1 to 2 μm. This study confirmed endothelial cells polarization along the grooves and significantly enhanced alignment on deeper grooves. Furthermore, it was illustrated that FA kinase mediates cell spreading, while cell alignment is dependent on ROCK1/2, myosin–II–mediated cell contractility, and FA maturation [89].

Subsequent works on cell–substrate interactions have focused on investigating cell morphology and adhesion on other types of topographical features including pillars [95–99], wells [100], pits [101,102], pyramidal-shaped microstructures [103], and isotropically-etched cavities with curved surfaces [104–108]. For instance, Turner et al. investigated the attachment of astroglial cells on microarrays of pillars for designing implantable neural devices [95]. The substrates were fabricated with silicon using photolithography and wet chemical etching. The width and spacing of the pillars was varied between 0.5–2 μm and 1–5 μm, respectively, and the height was 1 μm. Astroglial cells cultured on pillar geometries showed a significant tendency to adhere and exhibit highly polarized actin filaments and vinculin, a constituent of the FA complex. Studies by Frey et al. and Ghibaudo et al. demonstrated a branched morphology and FA stabilization in fibroblasts cultured on PS and PDMS pillars, respectively, both fabricated with soft lithographic techniques (Fig. 2c) [96,97]. The dimensions of the pillars, such as height and spacing, were shown to influence the cells' morphology and spreading. Decreasing pillar height led to cells exhibiting morphologies similar to being cultured on flat surfaces [97]. In another study, increasing the gap size between pillars was shown to significantly affect the morphology of fibroblasts, in which they adopted a more stellate-like shape accompanied by diffuse actin fibers and fewer FAs (Fig. 2d) [99]. On the other hand, for smaller gap sizes, the cell morphology was more similar to those on flat surfaces. Nikkhah et al. introduced the development of 3D isotropically-etched microstructures comprised of curved surfaces fabricated with silicon to study the adhesion and cytoskeletal organization of human fibroblasts, breast epithelial cells, and highly metastatic breast cancer cells (Fig. 2e–h) [104–108]. The depth of the etched microstructures varied between 60 and 70 μm and the width was in the range of 150–170 μm. Differential adhesion patterns of cells within the etched cavities was demonstrated; fibroblasts stretched, while the breast epithelial and metastatic breast cancer cells adopted the shape of the curved surfaces of the etched microstructures [104–106]. Further investigation confirmed that the cytoskeletal organization and biomechanical properties of the cells, as well as cell–cell junctions dictate the adhesion pattern

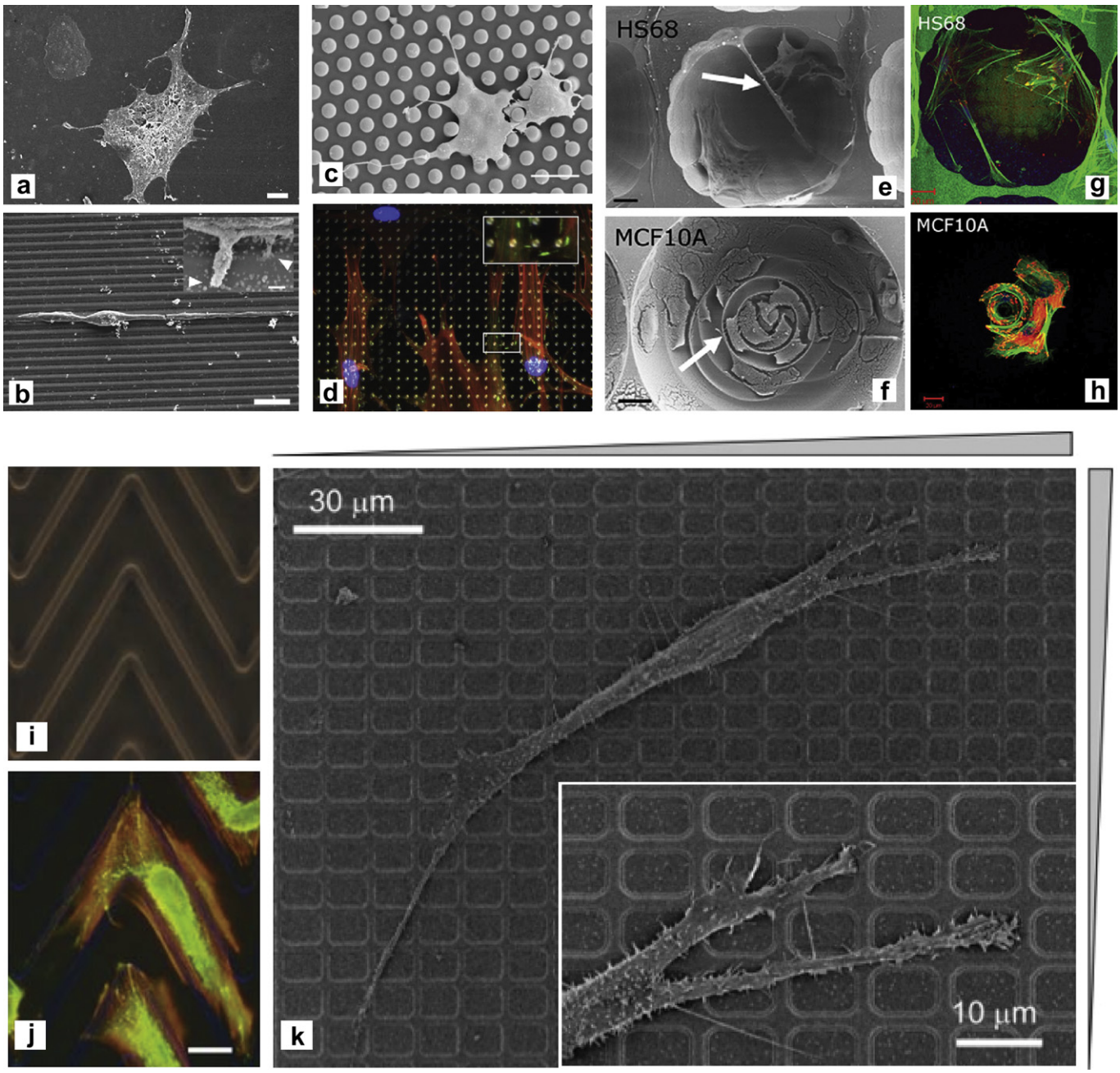

Fig. 2. Fabricated topographies for cell adhesion and migration analysis. (a,b) Scanning electron micrographs (SEM) of endothelial cells cultured on a flat PGS surface (a) and a microgrooved surface (b) demonstrating cellular alignment on microgrooves [88]. Scale bars, (a) 10 μm, (b) 10 μm and 1 μm for inset image. Adapted with permission from Elsevier: [Biomaterials], copyright (2006). (c) SEM image of the induced branched morphology of fibroblasts on array of PDMS micropillars [97]. Scale bar, 20 μm. Adapted with permission from Cell Press: [Biophysical Journal], copyright (2009). (d) Human skin fibroblasts on tantalum-coated silicon micropillars showing diffuse actin fibers (red fluorescent staining) and fewer FAs (green, vinculin fluorescent staining) [99]. Adapted with permission from Elsevier: [Biomaterials], copyright (2010). (e–h) SEM (e, f) and confocal fluorescent images (g, h) of fibroblasts (HS68) and human breast epithelial cells (MCF10A) attached within isotropically-etched silicon cavities fabricated [106]. Scale bar, 20 μm. Adapted with permission from Elsevier: [Biomaterials], copyright (2010). (i, j) Smooth muscle cell morphology and cytoskeleton followed the shape of PDMS zig-zag microstructure array that they were cultured on. Phase image of pattern (i) and merged fluorescent staining against actin (red) and vinculin (green) (j) [131]. Adapted with permission from Springer: [Biomedical Microdevices], copyright (2007). (k) Directional fibroblast migration on poly(urethane acrylate), rectangular lattice patterns as shown in these SEM images [133]. Adapted with permission from Wiley: [Advanced Functional Materials], copyright (2009). (For interpretation of the references to color in this figure legend, the reader is referred to the web version of this article.)

of a cell within the etched cavities [105,106]. Moreover, treatment of the breast cancer cells within the etched cavities with anti-cancer drugs induced a stretched morphology similar to the fibroblasts [107]. In co-culture of normal and cancerous breast epithelial cells, both cells adopted the shape of cavities. However, after anti-cancer drug treatment, only the breast epithelial cancer cells stretched [108].

While the previous studies illustrate the influence of substrate topography on cell morphology and adhesion, the response of cells to microscale topographies is highly dependent on the cell type, in addition to the geometry and dimension of the substrate's topography (Fig. 2i,j). Further comprehensive studies need to be undertaken in the future to better elucidate the biological mechanism governing a cell's morphological response to substrate topography.

4. Cell migration

Efficient migration requires an asymmetric cell morphology consisting of a leading and a trailing edge. Cell migration is intimately connected to the biochemical and biophysical cues present in the microenvironment. Persistently directional migration requires a motogen—a signal that activates a cell's internal motility machinery—along with an asymmetric external cue that guides the direction of movement [21]. The external cue may consist of soluble signals (chemotaxis) [109], tethered adhesion molecules (haptotaxis), substrate stiffness (durataxis), and an electrical field (electrotaxis). In general, it is understood that in these environments, cells migrate by exhibiting asymmetry with a leading protrusion rich in actin (lamellipodium), integrin-mediated attachment to adhesion molecules, and detachment of the trailing edge of the cell [110]. ECM topography is one of the many factors that can influence the orientation of cell migration. It is possible that the physical structure and geometry of the ECM restrict sites of adhesion and directs migration through contact guidance [21]. For instance, in breast cancer metastasis, collagen fibers that are radiating outward from the mammary glands are known to mediate the directional migration of highly tumorigenic cells into the surrounding tissue [111–113]. Although, there remains much work in understanding the intracellular molecular pathways involved, small GTPases of the Rho-family [114] and stabilization of actin filaments [115] at the leading edge of the cell are critical elements during migration. The increasing utilization of microfabrication techniques in the construction of substrates with unique topographies may yield answers to the underlying mechanisms behind cell migration. Microfabricated substrates with asymmetric topographies have been used to recapitulate the directional migration of cells mediated by ECM topography. Given that cell motility is of crucial importance in processes such as morphogenesis [14,116], embryonic development [117], wound healing [118], and cancer metastasis [119,120], discovering the regulatory effects of topography on migration will enable better understanding of the mechanisms behind these physiological and pathological states.

Many cell types including fibroblasts [91,121–125], oligodendrocytes [126], neurons [127], epithelial [128], endothelial [91,129], and smooth muscle cells [91] have been shown to migrate along grooved topography. It has been shown that the average migration speed of cells is higher on microgrooved substrates than on flat surfaces [123,124,128,129]. For instance, Doyle et al. fabricated fibrillar patterns of different widths through photoablation of a poly(vinyl alcohol)-coated glass substrate to imitate the fibrillar structure of the ECM [130]. Fibroblasts and human keratinocytes cultured on 1.5 μm-wide fibrillar patterns demonstrated a uniaxial phenotype, 2–3-fold higher migration speeds, and efficient cell leading edge protrusion and trailing edge retraction compared to flat, unpatterned substrates. Furthermore, among patterns with widths in the range of 1–40 μm, the highest migration speed was observed along 2.5 μm-wide lanes. In general, cells cultured on grooved-topographies exhibit a higher migration speeds on narrower grooves [129]. In groove microtopographies, ridge width has also been shown to affect cell migration velocity. In one study, groove topographies were micromachined from a titanium alloy (Ti4Al6V) with groove, ridge, and depth dimensions ranging from 5 to 30 μm [123]. Fibroblasts seeded on these substrates demonstrated oriented cell morphology parallel to the ridges' long axis and highest migration velocity on 5 μm-wide ridges.

Recent generations of substrate topographies have attempted to fabricate more biomimetic features for cell migration analysis. Whereas groove topography examines the presentation of cues in a unidirectional manner, lattice topography better simulates the *in vivo* microenvironment by presenting multi-directional cues. Cells cultured on lattices differentially elongate and migrate along the direction of the long side of rectangular grids, compared to square ones [131]. The effect is greater for lattices with higher lattice aspect ratio and when the grid size is smaller than the size of each individual cell [132]. Furthermore, there is an explicable link between these observations and the actomyosin machinery. In these lattice topographies, cells treated with a myosin II inhibitor, blebbistatin, lost their exquisite sensitivity to the underlying topography and simply extruded multiple, randomly-oriented protrusions [131]. Further studies have attempted to mimic the complexity of the structures exhibited by the ECM. Kim et al. designed 1.5 μm-wide poly(urethane acrylate) lattice micropatterns via UV-assisted capillary force lithography, with variable density and anisotropy, to guide migration and orientation of fibroblasts in a spatially desired manner (Fig. 2k) [133]. Fibroblasts preferentially migrated and with increased speeds along the higher anisotropy and toward the denser regions of the topographical features. The assembly of cells in a spatially-oriented fashion using the abovementioned microtopographies could be used to construct oriented cell monolayers for cell sheet tissue engineering [134].

One of the reasons for the failure of implanted biomedical devices is due to inflammatory and epithelial cell migration on the device. Hence, it is desirable to modify the surface of these devices to impede cell migration. While various surface chemistry methods have been explored for this purpose, topographical modifications have recently come into the spotlight. Using adjacent silicon dioxide flat and microgrooved surfaces fabricated via photolithography and DRIE, black tetra epidermal keratocytes were repelled from or allowed to traverse the microgrooves based on the groove width and the angle of approach of the cells toward the feature boundary [135,136].

Pillar topographies have also attracted significant attention to provide insight into mechanisms of cell migration [96,97,121,137]. Spatial organization and dimensions of pillars have been shown to affect the migrational behavior of cells [96,97]. For instance, fibroblasts were shown to follow zig-zag patterns with higher speeds and turn frequencies on 10 μm-diameter, 1.7 μm-high polystyrene pillars compared to flat surfaces. Stable FAs, FA kinases, and contractile forces generated by myosin II were the major mechanisms dictating the cell response on these micropillar features [96]. Cell migration has also been preferentially directed along the axis of greatest rigidity or increasing substrate stiffness. For instance, micropillars of oval cross-section exhibit stiffer properties along their major axis compared to minor axis, thereby creating a mechanically-anisotropic structure [137]. When Madin–Darby canine kidney epithelial cells were cultured on these substrates, migration was directed parallel to the direction of the long axis of the ovals. In another work, a micropillar array with an increasing stiffness gradient was constructed by increasing the diameter of each pillar across the array [138]. Bovine aortic endothelial cells migrated preferentially toward the stiffer micropillars. The previous examples demonstrate an *in vitro* model for the role of mechanical stiffness in guiding cell migration (durotaxis) [139].

One principal advantage of studying cell migration at the microscale level is to recognize the fundamental mechanisms of multicellular migration [7,17,28]. *In vivo,* many cell types do not migrate alone, but as a collective group, resulting in organized sheets or 3D cellular clusters [11]. Though the effects of topography on collective migration have been established, the dominant mechanism has yet to be identified. To understand this mechanism, it has become essential to integrate topographical features and cellular mechanical response through physical cues. For example, microgrooved topographies enhanced epithelial and fibroblast tissue alignment and migration speeds compared to flat surfaces [124,128]. Furthermore, the effects of these substrates on tissue

alignment and migration speeds were similar to the corresponding single cell behaviors.

5. Stem cell differentiation

There has been a remarkable growth in using embryonic and adult stem cells in tissue engineering given their self-renewal and differentiation capacities [140–143]. However, the inability to precisely control stem cell fate has been a limitation in realizing the therapeutic potential of these cells [144–146]. The *in vivo* microenvironment of stem cells contains highly dynamic and intricate biochemical and biophysical cues, each playing their own role or in combination to regulate stem cell renewal and differentiation [147–151]. Therefore, establishing an environment that mimics key features of the stem cell niche is essential to the study and modulation of specific cellular processes. Development of *in vitro* topographical cues provides a rapid and inexpensive alternative to better recapitulate the *in vivo* microenvironment and guide stem cell differentiation [87,152–157]. For instance, in a study by Seo et al., enhanced osteogenic differentiation of mesenchymal stem cells (MSCs) was observed on geometrically ordered lattice micropatterns [158]. An interval pattern of 3 μm showed significant upregulation of alkaline phosphatase after 6 days and type-I collagen and osteocalcin after 12 days, compared to flat surfaces. However, the interval range of 4–8 μm resulted in downregulation of osteogenic markers. Further investigations demonstrated that MSCs cultured on lattice topography showed enhanced FA maturation, actin cytoskeletal organization, and FA kinase phosphorylation through the ROCK-myosin II pathway, elucidating the biological mechanism that directs topography-mediated cellular differentiation [159]. In another study, neural stem cells (NSCs) were grown on different topographies in order to understand their influence on differentiation [160]. NSCs cultured on chitosan films (flat surface) preferentially differentiated into astrocytes, whereas those cultured on multi-tubule conduit structures (30–90 μm in diameter) showed a ~6.5-fold higher β-III tubulin-positive cells compared to the films, indicating greater neuronal differentiation.

Patterned micropillars with configurable heights and constant diameter have also been used to manipulate the mechanical regulation of human MSC differentiation (Fig. 3a) [151,156]. Varying the height of these posts changes their mechanical stiffness, with increasing height leading to decreased stiffness. Human MSCs grown on shorter microposts (0.97 μm), showed spread morphology, highly organized actin morphology, large FAs, and enhanced osteogenic markers. Conversely, human MSCs cultured on taller microposts (12.9 μm), exhibited round morphology,

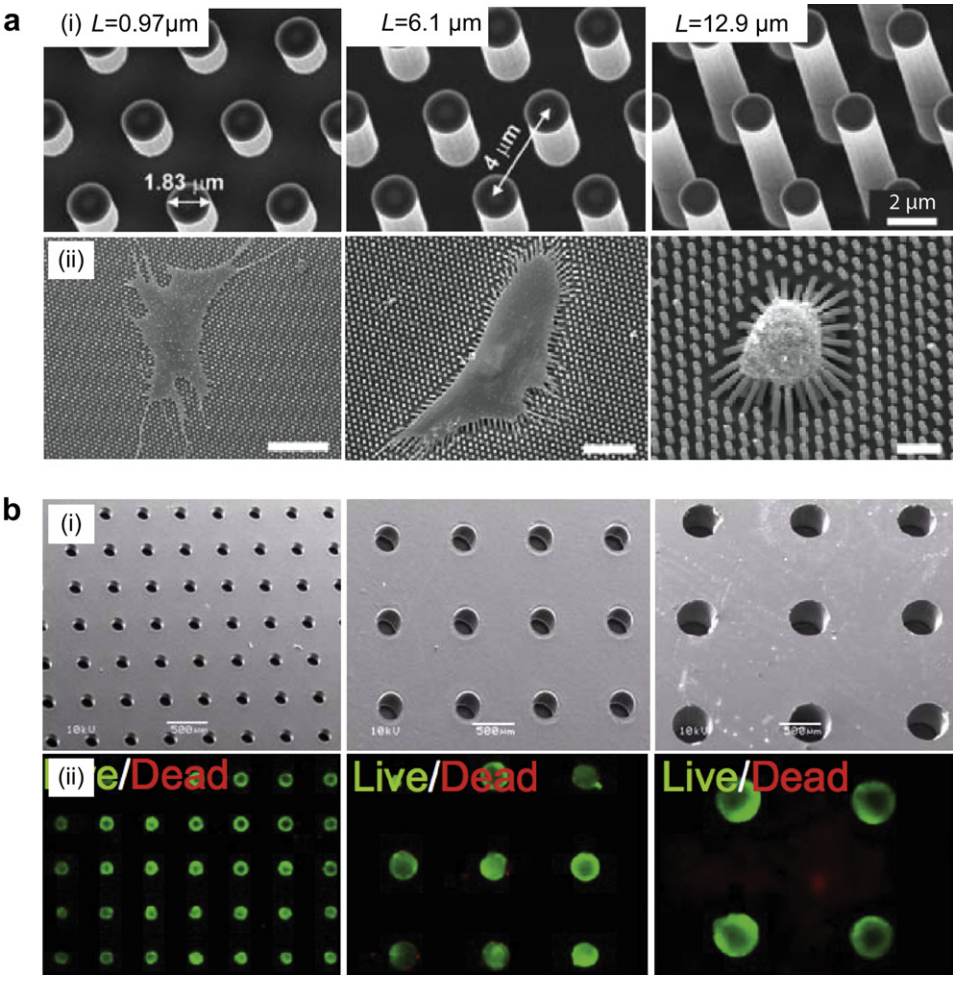

Fig. 3. Influence of topographical features on regulating stem cell fate. (a) The effect of stiffness on MSC morphology and differentiation using PDMS micropillars of varying heights as shown in these SEM images [151,156]. Scale bars, 50 μm (bottom left), 30 μm (bottom middle), 10 μm (bottom right). Adapted with permission from Macmillan Publishers Ltd: [Nature Protocols], copyright (2011). Adapted with permission from Macmillan Publishers Ltd: [Nature Methods], copyright (2010). (b) Formation of embryoid bodies (EBs) in poly(ethylene glycol) (PEG) hydrogel microwell arrays [162]. (bi) SEM images of uniform PEG microwell arrays with differing diameters (left = 150 μm, middle = 300 μm, right = 450 μm). (bii) fluorescent images of EBs formed within the microwells after 7 days. (Calcein-AM = green, ethidium homodimer = red). Copyright (2008) National Academy of sciences, USA. (For interpretation of the references to color in this figure legend, the reader is referred to the web version of this article.)

disorganized actin filaments, small FAs, and formation of lipid droplets, indicating adipogenesis. Similarly, PDMS microgrooves of different widths were used to investigate the differentiation capacity of umbilical cord blood-derived MSCs (UCB-MSCs) [161]. UCB-MSCs grown on 1 μm-wide grooves showed significant upregulation of β-III tubulin, neuronal nuclear antigen (NeuN), and microtubule associated protein 2 (MAP2) compared to wider grooves (2–4 μm widths) and flat surfaces, demonstrating that narrower grooves increase neuronal cell differentiation. Interestingly, UCB-MSCs on 1 μm grooves showed increased calcium levels in response to exogenous addition of potassium chloride, a characteristic response of mature neurons.

Recapitulation of the early steps of embryogenesis *in vitro* is commonly induced by the formation of 3D embryonic stem cell aggregates, called embryoid bodies (EBs). Microwells have become a common type of topography for generating EBs through favoring aggregation of ESCs [154,162–167]. In a work by Hwang et al., ESCs were seeded on poly(ethylene glycol) microwells with different diameters to study the size-dependent response of EBs on differentiation (Fig. 3b) [162]. The study demonstrated that EBs grown in larger microwells (450 μm diameter), exhibited preferential differentiation toward cardiogenesis through the expression of *Wnt11*. Conversely, EBs grown in smaller microwells (150 μm diameter) favored vascularization, mediated through *Wnt5a* expression. Additionally, other studies have demonstrated that microwell topographies are biomimetic microarchitectures in that they resemble the intestinal crypts. When Caco-2 cells, a type of small intestinal cells, were cultured on smaller microwells exhibited higher alkaline phosphatase activity compared to larger microwells, indicating enhanced differentiation toward intestinal epithelial cells [100].

Microtopographical cues allow for the precise control of physical stimuli for systematic differentiation of stem cells. In addition, such topographies enable improved understanding of how stem cells integrate the topographical information within their niche for the determination of their fate. Understanding the differentiation response of stem cells to physical stimulation will undoubtedly amplify the potential of using these cells for therapeutic applications in the near future.

6. Topography as a tool to study mechanobiology

The role of physical cues or mechanical forces in cell biology was first introduced in 1892 by Julius Wolff in describing the changes in bone structures in response to load bearing [168]. However, for much of the 20th century, the importance of mechanical forces was ignored as new molecular biology techniques emerged for the elucidation of the genetic and biochemical machinery of cells. Recently, with the advent of new technologies, microscale quantitative measurements of cellular forces have become a reality [26,28]. The re-emergence of cellular mechanics has been consequential in the study of biology and disease. Indeed, mechanical factors are present during embryogenesis and development [169], in adult life, and are involved in many pathological conditions [70], such as atherosclerosis [170], osteoporosis [171], myopathies [172], and cancer [173]. On a cellular level, there is mounting evidence that mechanical cues affect cellular proliferation [174], morphogenesis [175], migration [138], and stem cell differentiation [151,176]. These mechanical signals present themselves in the form of shear stress, hydrostatic pressure, ECM topography or stiffness, or intercellular tugging. Microtechnologies have enabled the fabrication of unique microtopographies, allowing for the study of physical cues provided by cell-substratum and cell–cell contacts. There are numerous other technologies currently being used for studying mechanobiology, including micropipette aspiration, optical or magnetic tweezers, and traction force microscopy [24]. However, whereas these techniques can be costly or low-throughput, microtopographies provide a cost-effective, accurate, high-throughput, and quantitative approach to mechanobiology.

One of the breakthroughs in studying cell mechanics through microtopographical features has been with the use of flexible micronscale post or pillar arrays [177]. These 3D geometrical microarrays are fabricated by photolithography and replica molding with the elastomer, PDMS. The surfaces of these arrays can be coated with ECM proteins via microcontact printing to render them cell-adhesive. As cells adhere to these arrays, they exert traction forces that cause a horizontal deflection on each pillar. In effect, each pillar behaves like a cantilever or a spring with spring constant, k. Its length of displacement, Δx, can be used to quantify the force, F, applied by the cell, as described by:

$$F = k \cdot \Delta x = \left(\frac{3}{4}\pi E \frac{r^4}{L^3}\right) \cdot \Delta x$$

where E is the Young's modulus, and r and L are the radius and height of each pillar, respectively (Fig. 4a) [178]. Micropillar arrays can be used to measure traction forces mediated through the FAs of a cell (Fig. 4b). The size of the FAs has been shown to be directly correlated with the traction force applied, when FA area is >1 μm^2 [177,179]. Further, the interdependency of FAs, cell morphology, and generated forces has been illustrated on micropillar arrays. Cells that were restricted from spreading, by controlling the area of cell adhesion on the arrays, did not contract in response to lysophosphatidic acid, a stimulant of actin-myosin contraction; however, contraction in unspread cells was rescued when they were transfected with constitutively active RhoA [177]. Mechanics of cell spreading can also be studied by widening the spacing between micropillars and allowing cell adhesion between them. In this environment, cells spread around the pillars and gradually apply increasing force on the pillars that they are in contact with, which was shown to be reversible with a myosin II inhibitor [180]. On flat PDMS surfaces, cells exhibited more actin stress fibers; however, in the 3D micropatterned environment, actin stress fibers were located to the parts of the cell surrounding the pillars. While micropillars are one way of inducing cells to apply differing traction forces, another method involves hydrogels with varying stiffness. However, the drawback is that the process of fabricating materials of varying stiffness results in the alteration of their other bulk material properties, such as porosity, ligand density, and wettability [156]. With micropillars, stiffness is decoupled from these other material properties that might influence cell behavior.

The transduction of mechanical forces not only involves FAs in cell-substratum interactions, but also adherens junctions (AJ) in cell–cell contact. AJ are protein complexes connecting one cell to another, and are linked to the actin-myosin cytoskeletal machinery. AJ are comprised of transmembrane proteins called cadherens, of which E-cadherin and N-cadherin have been well studied [181]. Mechanics in cell–cell contact plays an important role in embryo development and tissue morphogenesis [182,183]. For instance, it has been shown that epithelial sheet invagination occurs via the pulse contractions of actin and myosin underlying AJ [182]. Micropillars can be used to quantify the mechanical forces exerted by cells onto their neighboring cells. This can be accomplished in two ways. One is by the immobilization of cadherin molecules onto the top of the micropillar arrays. Using this method, Ganz et al. showed traction forces were greatest at the cell edges, directed toward the center of the cell, and similar in magnitude to those exerted by FAs [184]. In the second method,

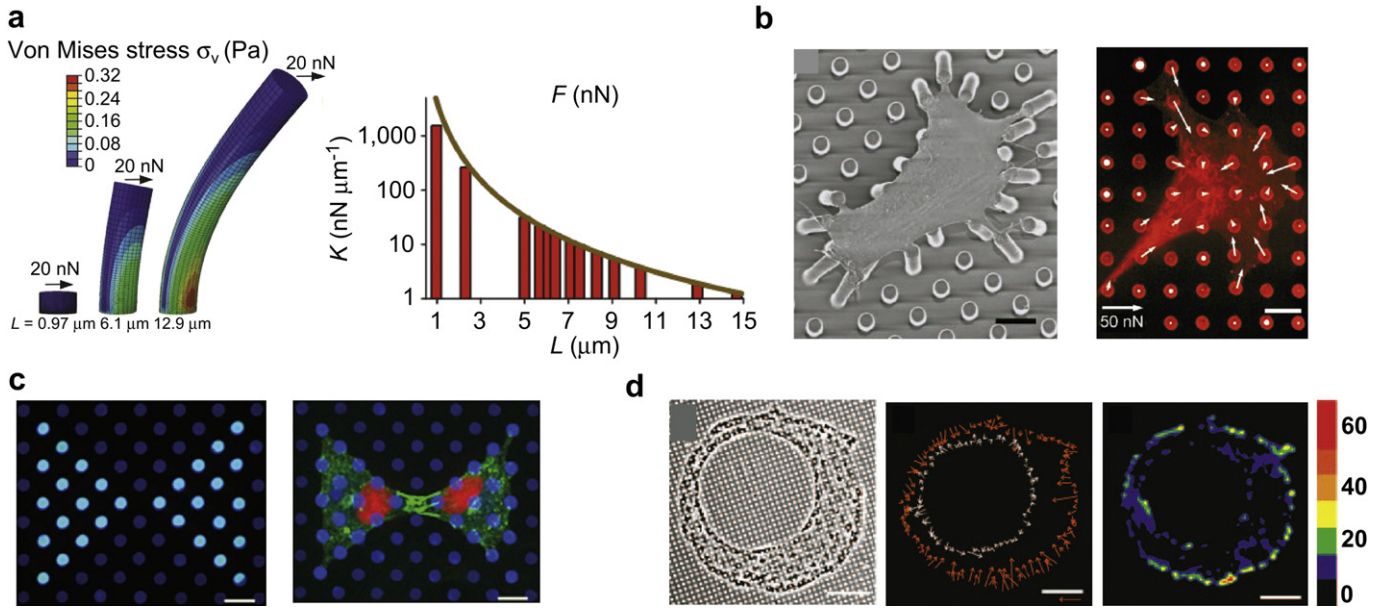

Fig. 4. Micropillar topographies to study cell-generated forces. (a) Micropillars of varying heights depicted using finite-element analysis and with spring constant, *K* [151]. Adapted with permission from Macmillan Publishers Ltd: [Nature Methods], copyright (2010). (b) Cell traction forces causing deflection of micropillars as shown in this SEM image (left) and immunofluorescent staining against fibronectin (right) [177]. The arrows indicate the magnitude of the traction forces. Scale bars, 10 μm. Copyright (2003) National Academy of Sciences, USA. (c) Cells cultured on micropillars to measure intercellular forces by constraining cell attachment sites on the pillars [185]. Fibronectin (cyan), nulei (red), and AJ (green) are shown. Scale bar, 10 μm. Copyright (2010) National Academy of Sciences, USA. (d) An anisotropic ring-shaped multicellular tissue constructed on micropillars to study the effect of mechanical forces on proliferation in tissues [174]. Images represent phase image (left), force vectors (middle), and colorimetric map of forces. Scale bar, 100 μm. Copyright (2005) National Academy of Sciences, USA. (For interpretation of the references to color in this figure legend, the reader is referred to the web version of this article.)

Liu et al. used a fibronectin-micropatterned pillars that permitted only a single contact between two cells, to measure the force exerted by one cell onto another, called the "tugging force" (Fig. 4c) [185]. At the quasi–static equilibrium state, the cells are assumed to be stationary, and hence the net force on a cell body is zero. This means that for an isolated stationary cell on a micropillar array, the net vector sum of the traction forces has to equal zero. However, a cell that is in contact with only a single cell on a micropillar array experiences not only traction forces, but also intercellular "tugging force" from its neighboring cell. Therefore, the vector sum of the traction forces and "tugging force" has to equal zero. The "tugging force" can then be derived, since traction forces can be calculated from pillar deflections. In the study, the size of AJ was directly correlated with the magnitude of the intercellular "tugging force" and was mediated by Rac pathway and actomyosin contractility.

While in the aforementioned examples internal cellular forces were measured, selective and precise application of external force on cells have been made possible with micropillar actuators. In these devices, magnetic materials (nanowires or nanoparticles) were incorporated into some or all of the micropillars. In the presence of an electric field, the magnetic micropillars applied force on cells cultured on them, while non-magnetic micropillars deflected in response to traction forces generated internally by the cell [186,187]. In this way, simultaneous monitoring of internal and external forces was accomplished. Application of an external force resulted in an increase in FAs at only the actuated posts, and a non-uniform loss of traction forces at the other areas of the cell [188]. These results demonstrate the interplay between external and internal forces, and suggest that cell response to external mechanical forces may adjust their internally generated forces.

In addition to studying the amount of force generated by cells on their substrate and adjacent cells, and applying forces onto cells, micropillars have also been used to measure the effect of mechanical forces on cell proliferation within multicellular aggregates (Fig. 4d) [174], platelet contractile forces during thrombus formation [189], forces generated by endothelial cells during leukocyte adhesion and transmigration [190], and studying traction forces generated by epithelial monolayers [191]. Furthermore, the geometry and dimension of the microposts can be altered to obtain substrates with anisotropic or varying stiffness to affect cell migration [138] and stem cell differentiation as previously mentioned.

7. Application of microtopography in tissue engineering

Microfabrication technologies have been proven to be powerful techniques in addressing the current challenges in tissue engineering [38]. To date, microfabrication technologies have been widely used in the development of substrates, scaffolds, or biomaterials comprised of precise topographical features to meet the desired criteria and complexity of the native tissue architecture. In the following sections, we will cover the application of microscale topographies in neural, cardiac and musculoskeletal tissue engineering fields.

7.1. Neural tissue engineering

In the developing nervous system, there exists a dynamic and highly organized histogenesis, whereby neurons have to forge specific connections to other neurons via their cellular projections (*i.e.* neurites including dendrites and axons), to generate the correct cellular circuitry [192]. The precise cellular migration and axon guidance are mediated through biochemical and biophysical cues present in the cell's microenvironment. For instance, neurons can sense and migrate along directed ECM fibers or glial cell tracts [193]. The sensitivity of neurons to the physical or topographical cues in their environment has been exploited both *in vitro* and *in vivo* for tissue engineering purposes [27,194]. *In vitro*, micro-topographical cues, such as grooves or pillars, have been developed

to guide and direct cellular behaviors such as neuronal cell and nuclear alignments, and axon guidance. Such cell culture platforms are not only beneficial in the development of models for nervous system biology, but also in creating therapeutic approaches for nerve injuries.

The *in vitro* studies of the effect of microtopography on neurons have consisted of using anisotropic or isotropic features, and quantifying cell or neurite alignments with the goal of directing neurite extension. Microgrooves of varying heights (2.5–69 μm), widths (5–350 μm), and spacings (20–60 μm) have been widely used in this context. In general, there is a greater degree of neurite alignment in deeper, narrower, and less spaced apart microgrooves [195–198]. Functionalization of these topographies with biomolecules, such as laminin or nerve growth factor [199], further enhances their effects on cell and neurite alignments. In work by Kang et al. embryonic neurons seeded on laminin-coated grooved fibers induced a higher degree of neurite extension compared to smooth fibers (Fig. 5ai) [200]. In the study, the fibers were

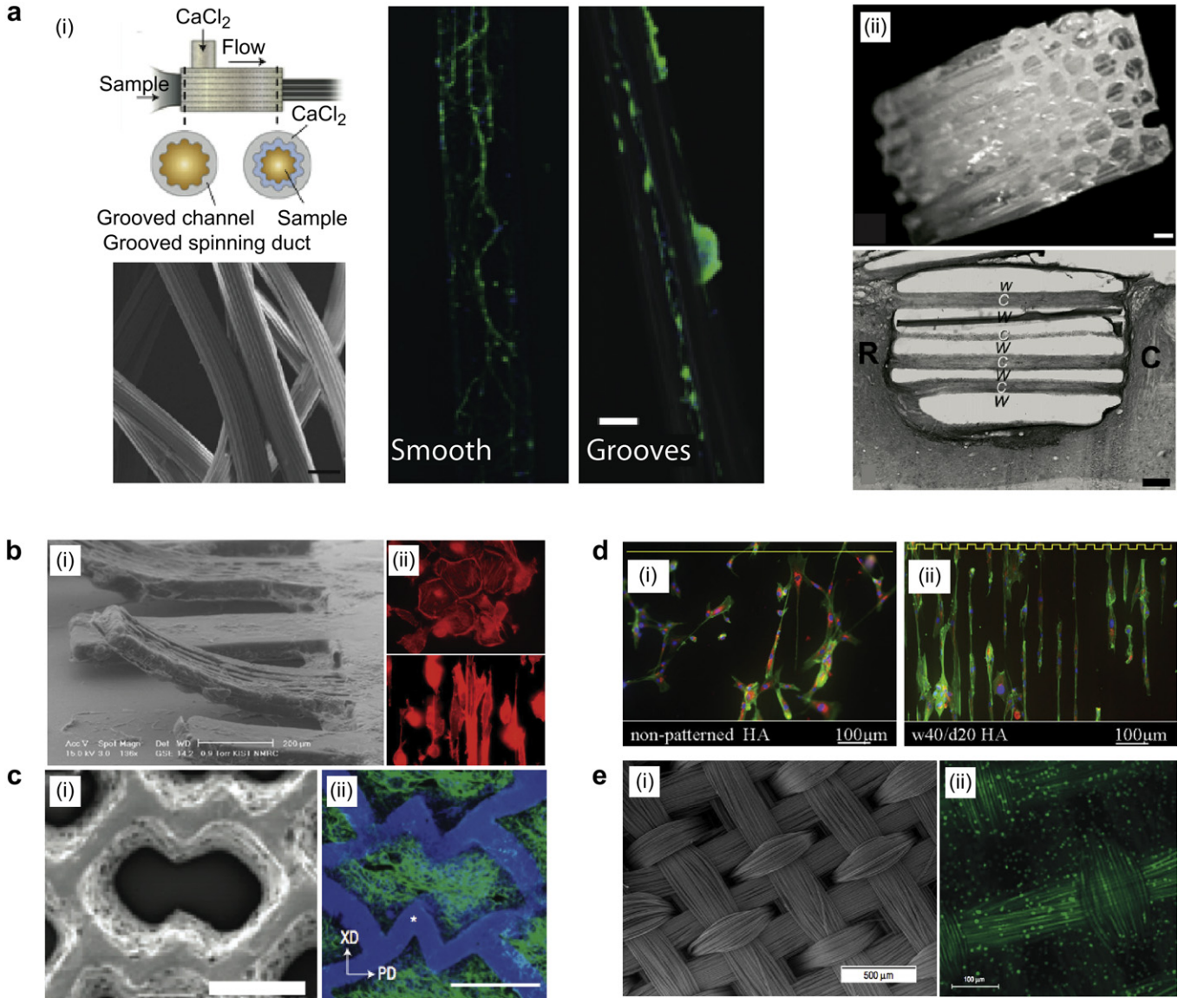

Fig. 5. (a) Topographical approaches to neural tissue engineering. (ai) Neurite alignment and extension of embryonic neurons is enhanced on grooved fibers compared to smooth fibers [200]. Shown are the schematic of the alginate hydrogel microfiber generation (top left), SEM image of the microfibers (bottom left), and fluorescent image of neurons seeded on smooth (middle) and grooved (right) microfibers (green, neurofilament; blue, nucleus). Scale bars, 20 μm (ai bottom left), 50 μm (ai right). (aii) Agarose conduits containing multiple micronscale channels (top) and Nissl staining (bottom) showing the growth of cells within channels (designated C) surrounded by the scaffold walls (designated W) [233]. Scale bars, 200 μm (aii top), 100 μm (aii bottom). Adapted with permission from Elsevier: [Biomaterials], copyright (2010). (b) Spatial arrangement of cardiomyocytes cultured on flat and grooved cantilevers [217]. (bi) Environmental SEM images of microcantilever structures with both flat and grooved surfaces. (bii) Morphological characteristics of cardiomyocytes visualized by actin (red) staining on flat (top) and grooved (bottom) microcantilevers. Adapted with permission from Elsevier: [Journal of Biomechanics], copyright (2008). (c) PGS honeycomb-shaped scaffold designed to closely mimic the mechanical properties of native myocardium [219]. (ci) SEM image of the scaffold. Scale bar, 200 μm. (cii) Rat cardiac cells cultured for 1 week on a honeycomb scaffold, showing cytoskeletal alignment (F-actin = green, nuclei = blue). The white asterisk indicates scaffold. Scale bar, 200 μm. Adapted with permission from Macmillan Publishers Ltd: [Nature Materials], copyright (2008). (d) Influence of microgroove topography on osteoblast shape and orientation [223]. Fluorescent images of osteoblasts cultured on flat hydroxyapatite (di) and 40 μm-wide grooved hydroxyapatite surfaces (dii) shown by phalloidin (green), collagen type-I (red), and DNA staining. Adapted with permission from Elsevier: [Acta Biomaterilia] copyright (2012). (e) 3D structure of woven poly(glycolic acid) yarn for generating a biomimetic scaffold for cartilage tissue engineering [228]. (ei) SEM images of fiber structures of the 3D woven composite scaffold. (eii) Calcein-AM stained porcine articular chondrocytes seeded on the construct. Adapted with permission from Macmillan Publishers Ltd: [Nature Materials], copyright (2007). (For interpretation of the references to color in this figure legend, the reader is referred to the web version of this article.)

generated through flowing alginate through a grooved PDMS channel with concomitant flow of calcium chloride as the cross-linking agent. Moreover, higher order structures can be formed by first culturing and aligning support cells on microgrooves, followed by seeding of neurons. In this regard, nerve growth factor-secreting cells [201], astrocytes [202], or Schwann cells [203], have been used as an intermediate layer between the topographical substrate and neurons, to induce neurite alignment or growth, or neuronal differentiation.

The control of the alignment of neurites and their growth in a desired direction is of particular interest in nervous system traumas, such as spinal cord injuries (SCI) [204,205]. In SCI, the injured axons encounter an inhibitory environment for growth that restricts their ability to make synapses with previously connected cells [206]. Hence, topographical guidance through nerve conduits has been one of the mainstream therapeutic interventions after SCI (Fig. 5aii). It is postulated that cells sense the curvature of these conduits as a form of a topographical cue. Engineering methods have been used to add topographical features inside these conduits in the hope of increasing permissive or inductive neurite guidance to promote nerve regeneration. These methods include fabricating conduits containing micrometer-sized channels or microgrooves within the lumen. Multichannel conduits have garnered increasing attention given that they increase the surface area for cell attachment, as well as enable an enhancement in the release of growth factors from the scaffold. Poly(lactic-*co*-glycolic acid) (PLGA) and polycaprolactone have been widely used as the choice of material given their ease of processing and biocompatibility. Furthermore, these synthetic materials allow for control over their architecture, porosity, and degradation rate [207,208]. In work by Krych et al., PLGA scaffolds containing multiple, parallel channels of either 450 μm- or 600 μm-diameter seeded with Schwann cells were implanted in the area of the transected spinal cord of an adult rat [209]. Scaffolds containing smaller diameter channels promoted greater nerve regeneration compared to the larger diameter channels. Similarly, Rutkowski et al. showed that the introduction of microgrooves in poly(D,L-lactic acid) conduits seeded with Schwann cells resulted in a more expeditious functional recovery in rats with transected sciatic nerves, compared to conduits without a microtopography [210]. These examples demonstrate the advantageous role of microtopography in engineered tissue engineered scaffolds and pave the way toward advancements in the field of nerve regeneration.

7.2. Cardiac tissue engineering

The native myocardial architecture embodies cellular alignment and organization which is closely linked to its proper functioning *in vivo* [211]. Microengineering of cardiac constructs aims to mimic the native cardiac tissue organization in an *in vitro* setting [35]. Precise control of biophysical environments has been widely utilized to recapitulate the native anisotropic structure of the myocardium and direct its behavior [211,212]. Studies have shown that topographical guidance can induce cardiomyocytes to resemble the *in vivo* phenotype and exhibit enhanced contractile activity [213–215].

In cardiac tissues, contractile properties are directly related to cellular orientation and elongation. Therefore, many studies have aimed to simulate the *in vivo* anisotropic structure of the myocardium through a series of topographical features with controllable mechanical properties. For example, Bursac et al. fabricated microabraded channels, 0.5–5 μm-wide and 0.2–2 μm in depth, on a poly(vinyl) chloride substrate that enabled cardiomyocyte alignment and resulted in an anisotropic structure [212]. Cardiomyocytes cultured on these microabrasions exhibited faster propagation of action potential along the long axis of abrasions. Furthermore, on these substrates, cells assembled into tissues exhibiting aligned actin fibers, parallel sarcomeric arrangements, and nuclear elongation, phenotypically mimicking the native *in vivo* structure. In another study by Yin et al. cardiomyocytes seeded on microgrooved substrates were shown to modify intracellular calcium behavior [216]. Cardiomyocytes cultured on microgrooved patterns exhibited increased systolic intracellular calcium and slower diastolic rise in calcium. Moreover, electrical stimulation led to increased systolic intracellular calcium at all stimulation frequencies and increased diastolic intracellular calcium at higher stimulation frequencies. These results demonstrate the effect of substrate changes on cardiomyocyte intracellular calcium dynamics and a possible model for cardiac arrhythmia. In another work, Kim et al. developed an analytical platform for measuring contractile forces generated by cardiomycytes cultured on flat and 10 μm-wide grooved cantilevers (Fig. 5b) [217]. Cardiomyocytes cultured on the cantilevers showed 3D aggregation accompanied with anisotropic actin organization and nuclear elongation. Furthermore, cardiomyocytes on grooved cantilevers had 65–85% higher contractile forces, compared to flat cantilevers, as measured through displacement of the cantilevers during contractions.

Topography has also been implemented in designing fully synchronous cardiac tissue constructs through gap junction formations and establishing interconnected networks of cardiomyocytes. In one study, cardiomyocytes grown on PDMS micropeg topographies of various dimensions and spacings were analyzed for junctional marker expressions [218]. The patterned topographies supported adhesion and growth of cardiomyocytes and a consistent contractile frequency across all micropeg configurations. Furthermore, dense and clustered micropeg arrangements showed significant upregulation of N-cadherin and connexin43—a gap junction protein crucial for synchronized contraction in cardiomyocytes—compared to sparse micropeg arrangements, revealing the influence of micropeg arrangements in propagation of electrical signaling and synchronous contractility of cardiac tissue constructs.

Engineered scaffolds have also shown a great promise in recapitulating the anisotropy and mechanical properties of the cardiac muscle tissues. For example, PGS scaffolds were constructed into an accordion-like honeycomb structure to obtain tensile properties similar to the ventricular myocardium (Fig. 5c) [219]. The anisotropic design of the scaffolds resulted in a lower cell shape index, exhibited by a significant increase in the degree of cardiomyocyte alignment when compared to an isotropic scaffold design. Furthermore, cardiomyocytes cultured on these scaffolds exhibited a directionally-dependent contractile behavior.

Understanding the characteristic morphology and cellular phenotype of cardiac cells and tissues directly influences the development of strategies to recapitulate the *in vivo* cellular environment. The phenotypic mimicry of cardiac muscles is coupled with increased contractile and electrical activity, allowing for more advanced cardiac tissue engineering platforms suitable toward clinical applications.

7.3. Musculoskeletal tissue engineering

Bones are highly vascularized tissues with an intrinsic capacity to remodel and self-heal. Currently, the gold standard for treating bone defects is through autologous bone grafts. However, this method has many disadvantages such as increased rates of infection, limited osteogenicity, and limited applicability to mild injuries [220]. These drawbacks have called for alternative treatment methods. One promising avenue is through engineering bone tissue

constructs that would require anisotropic mechanical properties, formation of oriented cells necessary for hierarchical organization, and mimicking the *in vivo* phenotype [221]. To fabricate such constructs, surface topography has been utilized to precisely control cellular orientation and alignment [80,222,223]. Kirmizidis et al. elucidated the role of surface topography as a modulator of primary osteoblast alignment by using microgroove patterns [224]. Osteoblasts grown on grooves of 7 μm depth and 10, 15, and 30 μm widths demonstrated predominant orientation along the grooves compared to flat surfaces. Moreover, osteoblasts grown on 10 μm-wide grooves formed multilayered structures validated by higher connexin43 gap junction size compared to flat surfaces. Further studies have confirmed that narrower microgrooves lead to an increase in cellular alignment of human osteoblasts [223]. Cellular orientation of osteoblasts between 0 and 15°—with zero degrees as the reference angle to the groove's long axis—was 64–79% on 20 μm-wide channels, while on 100 μm-wide channels only 29–47% osteoblasts alignment was present (Fig. 5d) [223]. Though significant progress has been achieved in the field of bone tissue engineering, future studies are aimed at improving osteoblast integration in constructs to improve the success of bone implants.

Unlike bone, cartilage has a limited number of cells and is avascular. However, due to its limited self-healing capacity and limited success of current clinical therapeutics, tissue engineering may serve as a suitable alternative for restoring cartilage [225]. *In vivo*, a vital requirement for cartilage formation is cellular aggregation of chondrocytes. The exploitation of surface topography has been used to physically induce aggregation of chondrocytes [226]. One study employed the use of microgroove topographies to influence aggregation of chondrocytes. Chondrocytes cultured on these microgrooves showed significantly increased cellular aggregation and directional migration along the groove's long axis compared to flat surfaces. Interestingly, grooves with greater depths (>3 μm) induced an organized multi-layer aggregation of chondrocytes, indicating the potential use of these topographical geometries as a tool for cartilage tissue formation [227].

A significant challenge of generating cartilage *in vitro* is mimicking its native structural and mechanical properties. *In vivo*, cartilage exhibits anisotropic and heterogeneous viscoelastic properties. Moutos et al. developed an anisotropic, 3D woven scaffold made out of 104 μm-diameter polyglycolic acid yarn that had similar compressive, tensile, and shear properties as that of native articular cartilage (Fig. 5e) [228]. Moreover, chondrocytes seeded on the oriented fibers of the scaffold exhibited a spatially uniform cellular distribution and rounded morphology, raising the possibility of using this construct for cartilage repair.

Currently, topographical features are being fabricated to mimic the tissue's native structural environment. Despite current progress, the field of musculoskeletal tissue engineering needs to make advancements toward emulating the overall physical characteristics of the native tissue to target repair and regeneration.

8. Conclusions and future prospects

Microfabrication technology has been proven to be a powerful tool to develop topographical features for mimicking the natural architecture of the ECM environment. Microscale topographical cues can be used to precisely control adhesion, morphology, migration, and differentiation in a wide variety of cell types ranging from fibroblasts to MSCs, as well as be applied to measure cell-generated forces.

Considering that previous studies have produced a large body of knowledge and have provided valuable insight into manipulating cell behavior through cell–substrate interactions, there are still several challenges within this field, which need to be addressed in the future. Further studies are required to elucidate the underlying molecular mechanism responsible for modulating cell–substrate interactions. For example, it would be crucial to identify signal transduction pathways which originate from cell attachment sites and govern gene expression and ultimately cell behavior. These findings will significantly enhance our knowledge in defining a general trend describing how substrate topography influences the behavior across different cell types rather than just comparing studies conducted on specific cells. Although, the majority of the previous works in this field have used simple topographical features such as grooves, future attempts should be more focused on realistic substrates with higher degree of biomimetic relevance to impose multi-directional cues within the cellular microenvironment. Such novel substrates will enable addressing questions on how cells globally integrate biophysical signals from their surrounding microenvironment. Furthermore, topographical features can be integrated with chemical stimuli, such as soluble factors, to enhance cellular process such as stem cell differentiation.

The continuous advancements in the field of cell–substrate topography interactions will not only benefit fundamental biological studies, but it will have significant implications in the field of tissue engineering through engineering synthetic and implantable substrates with controlled features.

Conflict of interest

The authors declare no competing interests.

Acknowledgments

The authors acknowledge funding from the National Science Foundation CAREER Award (DMR 0847287), the office of Naval Research Young National Investigator Award, and the National Institutes of Health (HL092836, DE019024, EB012597, AR057837, DE021468, HL099073, EB008392).

References

[1] Curtis A, Wilkinson C. Topographical control of cells. Biomaterials 1997;18:1573–83.
[2] Guck J, Lautenschlager F, Paschke S, Beil M. Critical review: cellular mechanobiology and amoeboid migration. Integr Biol (Camb) 2010;2:575–83.
[3] Hynes RO. The extracellular matrix: not just pretty fibrils. Science 2009;326:1216–9.
[4] Goodman SL, Sims PA, Albrecht RM. Three-dimensional extracellular matrix textured biomaterials. Biomaterials 1996;17:2087–95.
[5] Abrams GA, Goodman SL, Nealey PF, Franco M, Murphy CJ. Nanoscale topography of the basement membrane underlying the corneal epithelium of the rhesus macaque. Cell Tissue Res 2000;299:39–46.
[6] Pamula E, De Cupere V, Dufrene YF, Rouxhet PG. Nanoscale organization of adsorbed collagen: influence of substrate hydrophobicity and adsorption time. J Colloid Interface Sci 2004;271:80–91.
[7] Stevens MM, George JH. Exploring and engineering the cell surface interface. Science 2005;310:1135–8.
[8] Wang L, Carrier RL. In: George A, editor. Advances in biomimetics. Rijeka: InTech; 2011.
[9] Takahashi-Iwanaga H, Iwanaga T, Isayama H. Porosity of the epithelial basement membrane as an indicator of macrophage-enterocyte interaction in the intestinal mucosa. Arch Histol Cytol 1999;62:471–81.
[10] Takeuchi T, Gonda T. Distribution of the pores of epithelial basement membrane in the rat small intestine. J Vet Med Sci 2004;66:695–700.
[11] Rorth P. Whence directionality: guidance mechanisms in solitary and collective cell migration. Dev Cell 2011;20:9–18.
[12] Dent EW, Gertler FB. Cytoskeletal dynamics and transport in growth cone motility and axon guidance. Neuron 2003;40:209–27.
[13] Wolf K, Muller R, Borgmann S, Brocker EB, Friedl P. Amoeboid shape change and contact guidance: T-lymphocyte crawling through fibrillar collagen is independent of matrix remodeling by MMPs and other proteases. Blood 2003;102:3262–9.
[14] Haga H, Irahara C, Kobayashi R, Nakagaki T, Kawabata K. Collective movement of epithelial cells on a collagen gel substrate. Biophys J 2005;88:2250–6.
[15] Friedl P. Prespecification and plasticity: shifting mechanisms of cell migration. Curr Opin Cell Biol 2004;16:14–23.

[16] Campbell RD, Marcum BA. Nematocyte migation in hydra - evidence for contact guidance in vivo. J Cell Sci 1980;41:33–51.
[17] Eyckmans J, Boudou T, Yu X, Chen C. A hitchhiker's guide to mechanobiology. Dev Cell 2011;21:35–47.
[18] DuFort CC, Paszek MJ, Weaver VM. Balancing forces: architectural control of mechanotransduction. Nat Rev Mol Cell Biol 2011;12:308–19.
[19] Fletcher DA, Mullins RD. Cell mechanics and the cytoskeleton. Nature 2010; 463:485–92.
[20] Vogel V, Sheetz M. Local force and geometry sensing regulate cell functions. Nat Rev Mol Cell Biol 2006;7:265–75.
[21] Petrie RJ, Doyle AD, Yamada KM. Random versus directionally persistent cell migration. Nat Rev Mol Cell Biol 2009;10:538–49.
[22] Huang J, Grater SV, Corbellini F, Rinck S, Bock E, Kemkemer R, et al. Impact of order and disorder in RGD nanopatterns on cell adhesion. Nano Lett 2009;9: 1111–6.
[23] Park TH, Shuler ML. Integration of cell culture and microfabrication technology. Biotechnol Prog 2003;19:243–53.
[24] Moraes C, Sun Y, Simmons CA. (Micro)managing the mechanical microenvironment. Integr Biol (Camb) 2011;3:959–71.
[25] Bettinger CJ, Langer R, Borenstein JT. Engineering substrate topography at the micro- and nanoscale to control cell function. Angew Chem Int Ed Engl 2009;48:5406–15.
[26] Kim DH, Wong PK, Park J, Levchenko A, Sun Y. Microengineered platforms for cell mechanobiology. Annu Rev Biomed Eng 2009;11:203–33.
[27] Hoffman-Kim D, Mitchel JA, Bellamkonda RV. Topography, cell response, and nerve regeneration. Ann Rev Biomed Eng 2010;12:203–31.
[28] le Digabel J, Ghibaudo M, Trichet L, Richert A, Ladoux B. Microfabricated substrates as a tool to study cell mechanotransduction. Med Biol Eng Comput 2010;48:965–76.
[29] Flemming RG, Murphy CJ, Abrams GA, Goodman SL, Nealey PF. Effects of synthetic micro- and nano-structured surfaces on cell behavior. Biomaterials 1999;20:573–88.
[30] Takebe J, Champagne CM, Offenbacher S, Ishibashi K, Cooper LF. Titanium surface topography alters cell shape and modulates bone morphogenetic protein 2 expression in the J774A.1 macrophage cell line. J Biomed Mater Res A 2003;64A:207–16.
[31] Kunzler TP, Drobek T, Schuler M, Spencer ND. Systematic study of osteoblast and fibroblast response to roughness by means of surface-morphology gradients. Biomaterials 2007;28:2175–82.
[32] Tan KS, Qian L, Rosado R, Flood PM, Cooper LF. The role of titanium surface topography on J774A.1 macrophage inflammatory cytokines and nitric oxide production. Biomaterials 2006;27:5170–7.
[33] Lauer G, Wiedmann-Al-Ahmad M, Otten JE, Hubner U, Schmelzeisen R, Schilli W. The titanium surface texture effects adherence and growth of human gingival keratinocytes and human maxillar osteoblast-like cells in vitro. Biomaterials 2001;22:2799–809.
[34] Eisenbarth E, Meyle J, Nachtigall W, Breme J. Influence of the surface structure of titanium materials on the adhesion of fibroblasts. Biomaterials 1996;17:1399–403.
[35] Au HT, Cheng I, Chowdhury MF, Radisic M. Interactive effects of surface topography and pulsatile electrical field stimulation on orientation and elongation of fibroblasts and cardiomyocytes. Biomaterials 2007;28:4277–93.
[36] Anselme K, Bigerelle M, Noel B, Iost A, Hardouin P. Effect of grooved titanium substratum on human osteoblastic cell growth. J Biomed Mater Res 2002;60: 529–40.
[37] Castellani R, de Ruijter A, Renggli H, Jansen J. Response of rat bone marrow cells to differently roughened titanium discs. Clin Oral Implan Res 1999;10: 369–78.
[38] Khademhosseini A, Langer R, Borenstein J, Vacanti JP. Microscale technologies for tissue engineering and biology. Proc Natl Acad Sci U S A 2006;103: 2480–7.
[39] Madou MJ. Fundamentals of microfabrication: the science of miniaturization. Boca Raton: CRC Press; 2002.
[40] Franssila S. Introduction to microfabrication. West Sussex: Wiley Online Library; 2004.
[41] Song W, Lu H, Kawazoe N, Chen G. Adipogenic differentiation of individual mesenchymal stem cell on different geometric micropatterns. Langmuir 2011;27:6155–62.
[42] Bae H, Ahari AF, Shin H, Nichol JW, Hutson CB, Masaeli M, et al. Cell-laden microengineered pullulan methacrylate hydrogels promote cell proliferation and 3D cluster formation. Soft Matter 2011;7:1903–11.
[43] Qi H, Du Y, Wang L, Kaji H, Bae H, Khademhosseini A. Patterned differentiation of individual embryoid bodies in spatially organized 3D hybrid microgels. Adv Mater 2010;22:5276–81.
[44] Rothschild M. Projection optical lithography. Mater Today 2005;8:18–24.
[45] Yang S-P, Yang C-Y, Lee T-M, Lui T-S. Effects of calcium-phosphate topography on osteoblast mechanobiology determined using a cytodetacher. Mater Sci Eng C 2012;32:254–62.
[46] Revzin A, Tompkins RG, Toner M. Surface engineering with poly(ethylene glycol) photolithography to create high-density cell arrays on glass. Langmuir 2003;19:9855–62.
[47] Kovacs GTA, Maluf NI, Petersen KE. Bulk micromachining of silicon. Proc IEEE 1998;86:1536–51.
[48] Rangelow IW. Critical tasks in high aspect ratio silicon dry etching for microelectromechanical systems. J Vac Sci Technol A 2003;21:1550–62.
[49] Gantz K, Renaghan L, Agah M. Development of a comprehensive model for RIE-lag-based three-dimensional microchannel fabrication. J Micromech Microeng 2008;18:025003.
[50] Zellner P, Renaghan L, Hasnain Z, Agah M. A fabrication technology for three-dimensional micro total analysis systems. J Micromech Microeng 2010;20: 1–8.
[51] Hahn MS, Miller JS, West JL. Three dimensional biochemical and biomechanical patterning of hydrogels for guiding cell behavior. Adv Mater 2006; 18:2679–84.
[52] Mapili G, Lu Y, Chen S, Roy K. Laser-layered microfabrication of spatially patterned functionalized tissue-engineering scaffolds. J Biomed Mater Res B Appl Biomater 2005;75:414–24.
[53] Lan PX, Lee JW, Seol Y-J, Cho D-W. Development of 3D PPF/DEF scaffolds using micro-stereolithography and surface modification. J Mater Sci Mater Med 2009;20:271–9.
[54] Sun C, Fang N, Wu DM, Zhang X. Projection micro-stereolithography using digital micro-mirror dynamic mask. Sens Actuators A Phys 2005;121:113–20.
[55] Lee K-S, Kim RH, Yang D-Y, Park SH. Advances in 3D nano/microfabrication using two-photon initiated polymerization. Prog Polym Sci 2008;33:631–81.
[56] Seidlits SK, Schmidt CE, Shear JB. High-resolution patterning of hydrogels in three dimensions using direct-write photofabrication for cell guidance. Adv Funct Mater 2009;19:3543–51.
[57] Weibel DB, DiLuzio WR, Whitesides GM. Microfabrication meets microbiology. Nat Rev Micro 2007;5:209–18.
[58] Xia YN, Whitesides GM. Soft lithography. Angew Chem Int Ed Engl 1998;37: 551–75.
[59] Whitesides GM, Ostuni E, Takayama S, Jiang X, Ingber DE. Soft lithography in biology and biochemistry. Annu Rev Biomed Eng 2001;3:335–73.
[60] Zhong C, Kapetanovic A, Deng Y, Rolandi M. A chitin nanofiber ink for air-brushing, replica molding, and microcontact printing of self-assembled macro-, micro-, and nanostructures. Adv Mater 2011;23:4776–81.
[61] Xia YN, McClelland JJ, Gupta R, Qin D, Zhao XM, Sohn LL, et al. Replica molding using polymeric materials: a practical step toward nanomanufacturing. Adv Mater 1997;9:147–9.
[62] Whitesides GM. The origins and the future of microfluidics. Nature 2006; 442:368–73.
[63] Perl A, Reinhoudt DN, Huskens J. Microcontact printing: limitations and achievements. Adv Mater 2009;21:2257–68.
[64] Schwarz US, Bischofs IB. Physical determinants of cell organization in soft media. Med Eng Phys 2005;27:763–72.
[65] van der Flier A, Sonnenberg A. Function and interactions of integrins. Cell Tissue Res 2001;305:285–98.
[66] Tzima E, Irani-Tehrani M, Kiosses WB, Dejana E, Schultz DA, Engelhardt B, et al. A mechanosensory complex that mediates the endothelial cell response to fluid shear stress. Nature 2005;437:426–31.
[67] Hayakawa K, Tatsumi H, Sokabe M. Actin stress fibers transmit and focus force to activate mechanosensitive channels. J Cell Sci 2008;121:496–503.
[68] Giannone G, Sheetz MP. Substrate rigidity and force define form through tyrosine phosphatase and kinase pathways. Trends Cell Biol 2006;16: 213–23.
[69] Mitra SK, Hanson DA, Schlaepfer DD. Focal adhesion kinase: in command and control of cell motility. Nat Rev Mol Cell Biol 2005;6:56–68.
[70] Jaalouk DE, Lammerding J. Mechanotransduction gone awry. Nat Rev Mol Cell Biol 2009;10:63–73.
[71] Schwartz MA, Ginsberg MH. Networks and crosstalk: integrin signalling spreads. Nat Cell Biol 2002;4:E65–8.
[72] Hynes RO. Integrins: bidirectional, allosteric signaling machines. Cell 2002; 110:673–87.
[73] Riveline D, Zamir E, Balaban NQ, Schwarz US, Ishizaki T, Narumiya S, et al. Focal contacts as mechanosensors: externally applied local mechanical force induces growth of focal contacts by an mDia1-dependent and ROCK-independent mechanism. J Cell Biol 2001;153:1175–85.
[74] Discher DE, Janmey P, Wang YL. Tissue cells feel and respond to the stiffness of their substrate. Science 2005;310:1139–43.
[75] Ingber DE. Tensegrity: the architectural basis of cellular mechanotransduction. Annu Rev Physiol 1997;59:575–99.
[76] Rajnicek A, Britland S, McCaig C. Contact guidance of CNS neurites on grooved quartz: influence of groove dimensions, neuronal age and cell type. J Cell Sci 1997;110:2905–13.
[77] Karuri NW, Nealey PF, Murphy CJ, Albrecht RM. Structural organization of the cytoskeleton in SV40 human corneal epithelial cells cultured on nano- and microscale grooves. Microsc Microanal 2008;30:405–13.
[78] Oakley C, Brunette DM. The sequence of alignment of microtubules, focal contacts and actin-filaments in fibroblasts spreading on smooth and grooved titanium substrata. J Cell Sci 1993;106:343–54.
[79] Oakley C, Jaeger NAF, Brunette DM. Sensitivity of fibroblasts and their cytoskeletons to substratum topographies: topographic guidance and topographic compensation by micromachined grooves of different dimensions. Exp Cell Res 1997;234:413–24.
[80] Lu X, Leng Y. Quantitative analysis of osteoblast behavior on microgrooved hydroxyapatite and titanium substrata. J Biomed Mater Res A 2003;66A: 677–87.
[81] Scheideler L, Geis-Gerstorfer J, Kern D, Pfeiffer F, Rupp F, Weber H, et al. Investigation of cell reactions to microstructured implant surfaces. Mater Sci Eng C Mater Biol Appl 2003;23:455–9.

[82] Lu X, Leng Y. Comparison of the osteoblast and myoblast behavior on hydroxyapatite microgrooves. J Biomed Mater Res B Appl Biomater 2009; 90B:438–45.
[83] Clark P, Connolly P, Curtis ASG, Dow JAT, Wilkinson CDW. Topographical control of cell behavior: II. multiple grooved substrata. Development 1990; 108:635–44.
[84] Walboomers XF, Croes HJE, Ginsel LA, Jansen JA. Contact guidance of rat fibroblasts on various implant materials. J Biomed Mater Res 1999;47:204–12.
[85] Walboomers XF, Monaghan W, Curtis ASG, Jansen JA. Attachment of fibroblasts on smooth and microgrooved polystyrene. J Biomed Mater Res 1999; 46:212–20.
[86] Li JM, McNally H, Shi R. Enhanced neurite alignment on micro-patterned poly-L-lactic acid films. J Biomed Mater Res A 2008;87A:392–404.
[87] Charest JL, Garcia AJ, King WP. Myoblast alignment and differentiation on cell culture substrates with microscale topography and model chemistries. Biomaterials 2007;28:2202–10.
[88] Bettinger CJ, Orrick B, Misra A, Langer R, Borenstein JT. Micro fabrication of poly (glycerol-sebacate) for contact guidance applications. Biomaterials 2006;27:2558–65.
[89] Franco D, Klingauf M, Bednarzik M, Cecchini M, Kurtcuoglu V, Gobrecht J, et al. Control of initial endothelial spreading by topographic activation of focal adhesion kinase. Soft Matter 2011;7:7313–24.
[90] Uttayarat P, Toworfe GK, Dietrich F, Lelkes PI, Composto RJ. Topographic guidance of endothelial cells on silicone surfaces with micro- to nanogrooves: orientation of actin filaments and focal adhesions. J Biomed Mater Res A 2005;75A:668–80.
[91] Biela SA, Su Y, Spatz JP, Kemkemer R. Different sensitivity of human endothelial cells, smooth muscle cells and fibroblasts to topography in the nano-micro range. Acta Biomater 2009;5:2460–6.
[92] den Braber ET, de Ruijter JE, Smits HTJ, Ginsel LA, von Recum AF, Jansen JA. Quantitative analysis of cell proliferation and orientation on substrata with uniform parallel surface micro-grooves. Biomaterials 1996;17:1093–9.
[93] den Braber ET, de Ruijter JE, Ginsel LA, von Recum AF, Jansen JA. Orientation of ECM protein deposition, fibroblast cytoskeleton, and attachment complex components on silicone microgrooved surfaces. J Biomed Mater Res 1998;40: 291–300.
[94] Teixeira AI, Abrams GA, Bertics PJ, Murphy CJ, Nealey PF. Epithelial contact guidance on well-defined micro- and nanostructured substrates. J Cell Sci 2003;116:1881–92.
[95] Turner AMP, Dowell N, Turner SWP, Kam L, Isaacson M, Turner JN, et al. Attachment of astroglial cells to microfabricated pillar arrays of different geometries. J Biomed Mater Res 2000;51:430–41.
[96] Frey MT, Tsai IY, Russell TP, Hanks SK, Wang YL. Cellular responses to substrate topography: role of myosin II and focal adhesion kinase. Biophys J 2006;90:3774–82.
[97] Ghibaudo M, Trichet L, Le Digabel J, Richert A, Hersen P, Ladoux B. Substrate topography induces a crossover from 2D to 3D behavior in fibroblast migration. Biophys J 2009;97:357–68.
[98] Kidambi S, Udpa N, Schroeder SA, Findlan R, Lee I, Chan C. Cell adhesion on polyelectrolyte multilayer coated polydimethylsiloxane surfaces with varying topographies. Tissue Eng 2007;13:2105–17.
[99] Kolind K, Dolatshahi-Pirouz A, Lovmand J, Pedersen FS, Foss M, Besenbacher F. A combinatorial screening of human fibroblast responses on micro-structured surfaces. Biomaterials 2010;31:9182–91.
[100] Wang L, Murthy SK, Fowle WH, Barabino GA, Carrier RL. Influence of microwell biomimetic topography on intestinal epithelial Caco-2 cell phenotype. Biomaterials 2009;30:6825–34.
[101] Wan YQ, Wang Y, Liu ZM, Qu X, Han BX, Bei JZ, et al. Adhesion and proliferation of OCT-1 osteoblast-like cells on micro- and nano-scale topography structured pply(L-lactide). Biomaterials 2005;26:4453–9.
[102] Hamilton DW, Chehroudi B, Brunette DM. Comparative response of epithelial cells and osteoblasts to microfabricated tapered pit topographies in vitro and in vivo. Biomaterials 2007;28:2281–93.
[103] Le Saux G, Magenau A, Boecking T, Gaus K, Gooding JJ. The relative importance of topography and RGD ligand density for endothelial cell adhesion. Plos One 2011;6:e21869.
[104] Nikkhah M, Strobl JS, Agah M. Attachment and response of human fibroblast and breast cancer cells to three dimensional silicon microstructures of different geometries. Biomed Microdevices 2009;11:429–41.
[105] Nikkhah M, Strobl JS, Peddi B, Agah M. Cytoskeletal role in differential adhesion patterns of normal fibroblasts and breast cancer cells inside silicon microenvironments. Biomed Microdevices 2009;11:585–95.
[106] Nikkhah M, Strobl JS, De Vita R, Agah M. The cytoskeletal organization of breast carcinoma and fibroblast cells inside three dimensional (3-D) isotropic silicon microstructures. Biomaterials 2010;31:4552–61.
[107] Strobl JS, Nikkhah M, Agah M. Actions of the anti-cancer drug suberoylanilide hydroxamic acid (SAHA) on human breast cancer cytoarchitecture in silicon microstructures. Biomaterials 2010;31:7043–50.
[108] Nikkhah M, Strobl JS, Schmelz EM, Roberts PC, Zhou H, Agah M. MCF10A and MDA-MB-231 human breast basal epithelial cell co-culture in silicon microarrays. Biomaterials 2011;32:7625–32.
[109] Van Haastert PJM, Devreotes PN. Chemotaxis: signalling the way forward. Nat Rev Mol Cell Biol 2004;5:626–34.
[110] Ridley AJ, Schwartz MA, Burridge K, Firtel RA, Ginsberg MH, Borisy G, et al. Cell migration: integrating signals from front to back. Science 2003;302:1704–9.
[111] Sidani M, Wyckoff J, Xue C, Segall J, Condeelis J. Probing the microenvironment of mammary tumors using multiphoton microscopy. J Mammary Gland Biol Neoplasia 2006;11:151–63.
[112] Provenzano PP, Inman DR, Eliceiri KW, Knittel JG, Yan L, Rueden CT, et al. Collagen density promotes mammary tumor initiation and progression. BMC Med 2008;6:11.
[113] Provenzano PP, Inman DR, Eliceiri KW, Trier SM, Keely PJ. Contact guidance mediated three-dimensional cell migration is regulated by Rho/ROCK-dependent matrix reorganization. Biophys J 2008;95:5374–84.
[114] Jaffe AB, Hall A. Rho GTPases: biochemistry and biology. Annu Rev Cell Dev Biol 2005;21:247–69.
[115] Hotulainen P, Lappalainen P. Stress fibers are generated by two distinct actin assembly mechanisms in motile cells. J Cell Biol 2006;173:383–94.
[116] Huang S, Brangwynne CP, Parker KK, Ingber DE. Symmetry-breaking in mammalian cell cohort migration during tissue pattern formation: role of random-walk persistence. Cell Motil Cytoskel 2005;61:201–13.
[117] Helle T, Deiss S, Schwarz U, Schlosshauer B. Glial and neuronal regulation of the lipid carrier R-FABP. Exp Cell Res 2003;287:88–97.
[118] Maheshwari G, Wells A, Griffith LG, Lauffenburger DA. Biophysical integration of effects of epidermal growth factor and fibronectin on fibroblast migration. Biophys J 1999;76:2814–23.
[119] Bashyam MD. Understanding cancer metastasis. Cancer 2002;94:1821–9.
[120] Wells A. Tumor invasion: role of growth factor-induced cell motility. Adv Cancer Res 2000;78:31–101.
[121] Tzvetkova-Chevolleau T, Stephanou A, Fuard D, Ohayon J, Schiavone P, Tracqui P. The motility of normal and cancer cells in response to the combined influence of the substrate rigidity and anisotropic microstructure. Biomaterials 2008;29:1541–51.
[122] Kaiser JP, Bruinink A. Investigating cell-material interactions by monitoring and analysing cell migration. J Mater Sci Mater Med 2004;15:429–35.
[123] Kaiser J-P, Reinmann A, Bruinink A. The effect of topographic characteristics on cell migration velocity. Biomaterials 2006;27:5230–41.
[124] Kim D-H, Han K, Gupta K, Kwon KW, Suh K-Y, Levchenko A. Mechanosensitivity of fibroblast cell shape and movement to anisotropic substratum topography gradients. Biomaterials 2009;30:5433–44.
[125] Thampatty BP, Wang JHC. A new approach to study fibroblast migration. Cell Motil Cytoskel 2007;64:1–5.
[126] Webb A, Clark P, Skepper J, Compston A, Wood A. Guidance of oligodendrocytes and their progenitors by substratum topography. J Cell Sci 1995; 108:2747–60.
[127] Gomez N, Chen S, Schmidt CE. Polarization of hippocampal neurons with competitive surface stimuli: contact guidance cues are preferred over chemical ligands. J R Soc Interface 2007;4:223–33.
[128] Dalton BA, Walboomers XF, Dziegielewski M, Evans MDM, Taylor S, Jansen JA, et al. Modulation of epithelial tissue and cell migration by microgrooves. J Biomed Mater Res 2001;56:195–207.
[129] Li S, Bhatia S, Hu YL, Shin YT, Li YS, Usami S, et al. Effects of morphological patterning on endothelial cell migration. Biorheology 2001;38:101–8.
[130] Doyle AD, Wang FW, Matsumoto K, Yamada KM. One-dimensional topography underlies three-dimensional fibrillar cell migration. J Cell Biol 2009;184:481–90.
[131] Mai JY, Sun C, Li S, Zhang X. A microfabricated platform probing cytoskeleton dynamics using multidirectional topographical cues. Biomed Microdevices 2007;9:523–31.
[132] Jeon H, Hidai H, Hwang DJ, Healy KE, Grigoropoulos CP. The effect of micronscale anisotropic cross patterns on fibroblast migration. Biomaterials 2010;31:4286–95.
[133] Kim D-H, Seo C-H, Han K, Kwon KW, Levchenko A, Suh K-Y. Guided cell migration on microtextured substrates with variable local density and anisotropy. Adv Funct Mater 2009;19:1579–86.
[134] Isenberg BC, Tsuda Y, Williams C, Shimizu T, Yamato M, Okano T, et al. A thermoresponsive, microtextured substrate for cell sheet engineering with defined structural organization. Biomaterials 2008;29:2565–72.
[135] Miyoshi H, Ju J, Lee SM, Cho DJ, Ko JS, Yamagata Y, et al. Control of highly migratory cells by microstructured surface based on transient change in cell behavior. Biomaterials 2010;31:8539–45.
[136] Miyoshi H, Adachi T, Ju J, Lee SM, Cho DJ, Ko JS, et al. Characteristics of motility-based filtering of adherent cells on microgrooved surfaces. Biomaterials 2012;33:395–401.
[137] Saez A, Ghibaudo M, Buguin A, Silberzan P, Ladoux B. Rigidity-driven growth and migration of epithelial cells on microstructured anisotropic substrates. Proc Natl Acad Sci U S A 2007;104:8281–6.
[138] Sochol RD, Higa AT, Janairo RRR, Li S, Lin L. Unidirectional mechanical cellular stimuli via micropost array gradients. Soft Matter 2011;7:4606–9.
[139] Lo C-M, Wang H-B, Dembo M, Wang Y-l. Cell movement is guided by the rigidity of the substrate. Biophys J 2000;79:144–52.
[140] Guilak F, Cohen DM, Estes BT, Gimble JM, Liedtke W, Chen CS. Control of stem cell fate by physical interactions with the extracellular matrix. Cell Stem Cell 2009;5:17–26.
[141] Béduer A, Vieu C, Arnauduc F, Sol J-C, Loubinoux I, Vaysse L. Engineering of adult human neural stem cells differentiation through surface micropatterning. Biomaterials 2012;33:504–14.
[142] Buxboim A, Discher DE. Stem cells feel the difference. Nat Methods 2010;7: 695–7.
[143] Zemel A, Rehfeldt F, Brown AE, Discher DE, Safran SA. Optimal matrix rigidity for stress fiber polarization in stem cells. Nat Phys 2010;6:468–73.

[144] Discher DE, Mooney DJ, Zandstra PW. Growth factors, matrices, and forces combine and control stem cells. Science 2009;324:1673–7.
[145] Peerani R, Zandstra PW. Enabling stem cell therapies through synthetic stem cell-niche engineering. J Clin Invest 2010;120:60–70.
[146] Dellatore SM, Garcia AS, Miller WM. Mimicking stem cell niches to increase stem cell expansion. Curr Opin Biotechnol 2008;19:534–40.
[147] Edalat F, Bae H, Manoucheri S, Cha JM, Khademhosseini A. Engineering approaches toward deconstructing and controlling the stem cell environment. Ann Biomed Eng; 2011. doi:10.1007/s10439-011-0452-9.
[148] Chai C, Leong KW. Biomaterials approach to expand and direct differentiation of stem cells. Mol Ther 2007;15:467–80.
[149] Tsuruma A, Tanaka M, Yamamoto S, Shimomura M. Control of neural stem cell differentiation on honeycomb films. Colloids Surf A Physicochem Eng Asp 2008;313–314:536–40.
[150] Myllymaa S, Kaivosoja E, Myllymaa K, Sillat T, Korhonen H, Lappalainen R, et al. Adhesion, spreading and osteogenic differentiation of mesenchymal stem cells cultured on micropatterned amorphous diamond, titanium, tantalum and chromium coatings on silicon. J Mater Sci Mater Med 2010;21:329–41.
[151] Fu J, Wang YK, Yang MT, Desai RA, Yu X, Liu Z, et al. Mechanical regulation of cell function with geometrically modulated elastomeric substrates. Nat Methods 2010;7:733–6.
[152] Lim JY, Donahue HJ. Cell sensing and response to micro- and nanostructured surfaces produced by chemical and topographic patterning. Tissue Eng 2007;13:1879–91.
[153] Dickinson LE, Kusuma S, Gerecht S. Reconstructing the differentiation niche of embryonic stem cells using biomaterials. Macromol Biosci 2011;11:36–49.
[154] Moeller HC, Mian MK, Shrivastava S, Chung BG, Khademhosseini A. A microwell array system for stem cell culture. Biomaterials 2008;29:752–63.
[155] Markert LD, Lovmand J, Foss M, Lauridsen RH, Lovmand M, Fuchtbauer EM, et al. Identification of distinct topographical surface microstructures favoring either undifferentiated expansion or differentiation of murine embryonic stem cells. Stem Cells Dev 2009;18:1331–42.
[156] Yang MT, Fu J, Wang YK, Desai RA, Chen CS. Assaying stem cell mechanobiology on microfabricated elastomeric substrates with geometrically modulated rigidity. Nat Protoc 2011;6:187–213.
[157] Guvendiren M, Burdick JA. The control of stem cell morphology and differentiation by hydrogel surface wrinkles. Biomaterials 2010;31:6511–8.
[158] Seo CH, Furukawa K, Suzuki Y, Kasagi N, Ichiki T, Ushida T. A topographically optimized substrate with well-ordered lattice micropatterns for enhancing the osteogenic differentiation of murine mesenchymal stem cells. Macromol Biosci 2011;11:938–45.
[159] Seo CH, Furukawa K, Montagne K, Jeong H, Ushida T. The effect of substrate microtopography on focal adhesion maturation and actin organization via the RhoA/ROCK pathway. Biomaterials 2011;32:9568–75.
[160] Wang G, Ao Q, Gong K, Wang A, Zheng L, Gong Y, et al. The effect of topology of chitosan biomaterials on the differentiation and proliferation of neural stem cells. Acta Biomater 2010;6:3630–9.
[161] Kim SJ, Lee JK, Kim JW, Jung JW, Seo K, Park SB, et al. Surface modification of polydimethylsiloxane (PDMS) induced proliferation and neural-like cells differentiation of umbilical cord blood-derived mesenchymal stem cells. J Mater Sci Mater Med 2008;19:2953–62.
[162] Hwang YS, Chung BG, Ortmann D, Hattori N, Moeller HC, Khademhosseini A. Microwell-mediated control of embryoid body size regulates embryonic stem cell fate via differential expression of WNT5a and WNT11. Proc Natl Acad Sci U S A 2009;106:16978–83.
[163] Karp JM, Yeh J, Eng G, Fukuda J, Blumling J, Suh KY, et al. Controlling size, shape and homogeneity of embryoid bodies using poly(ethylene glycol) microwells. Lab Chip 2007;7:786–94.
[164] Khademhosseini A, Ferreira L, Blumling Jr , Yeh J, Karp JM, Fukuda J, et al. Co-culture of human embryonic stem cells with murine embryonic fibroblasts on microwell-patterned substrates. Biomaterials 2006;27:5968–77.
[165] Selimovic S, Piraino F, Bae H, Rasponi M, Redaelli A, Khademhosseini A. Microfabricated polyester conical microwells for cell culture applications. Lab Chip 2011;11:2325–32.
[166] Tekin H, Anaya M, Brigham MD, Nauman C, Langer R, Khademhosseini A. Stimuli-responsive microwells for formation and retrieval of cell aggregates. Lab Chip 2010;10:2411–8.
[167] Purpura KA, Bratt-Leal AM, Hammersmith KA, McDevitt TC, Zandstra PW. Systematic engineering of 3D pluripotent stem cell niches to guide blood development. Biomaterials 2012;33:1271–80.
[168] Wolff Y. Das gesetz der transformation der knochen. Berlin: Verlag von August Hirschwald; 1892.
[169] Yashiro K, Shiratori H, Hamada H. Haemodynamics determined by a genetic programme govern asymmetric development of the aortic arch. Nature 2007;450:285–8.
[170] Hahn C, Schwartz MA. Mechanotransduction in vascular physiology and atherogenesis. Nat Rev Mol Cell Biol 2009;10:53–62.
[171] Jacobs CR, Temiyasathit S, Castillo AB. Osteocyte mechanobiology and pericellular mechanics. Annu Rev Biomed Eng 2010;12:369–400.
[172] Chandrasekharan K, Martin PT. Genetic defects in muscular dystrophy. Methods Enzymol; 2010:291–322.
[173] Yu H, Mouw JK, Weaver VM. Forcing form and function: biomechanical regulation of tumor evolution. Trends Cell Biol 2011;21:47–56.
[174] Nelson CM, Jean RP, Tan JL, Liu WF, Sniadecki NJ, Spector AA, et al. Emergent patterns of growth controlled by multicellular form and mechanics. Proc Natl Acad Sci U S A 2005;102:11594–9.
[175] Kilian KA, Bugarija B, Lahn BT, Mrksich M. Geometric cues for directing the differentiation of mesenchymal stem cells. Proc Natl Acad Sci U S A 2010;107:4872–7.
[176] Gilbert PM, Havenstrite KL, Magnusson KEG, Sacco A, Leonardi NA, Kraft P, et al. Substrate elasticity regulates skeletal muscle stem cell self-renewal in culture. Science 2010;329:1078–81.
[177] Tan JL, Tien J, Pirone DM, Gray DS, Bhadriraju K, Chen CS. Cells lying on a bed of microneedles: an approach to isolate mechanical force. Proc Natl Acad Sci U S A 2003;100:1484–9.
[178] Crandall SH. An introduction to the mechanics of solids. New York: McGraw-Hill; 1978.
[179] Balaban NQ, Schwarz US, Riveline D, Goichberg P, Tzur G, Sabanay I, et al. Force and focal adhesion assembly: a close relationship studied using elastic micropatterned substrates. Nat Cell Biol 2001;3:466–72.
[180] Ghibaudo M, Di Meglio J-M, Hersen P, Ladoux B. Mechanics of cell spreading within 3D-micropatterned environments. Lab Chip 2011;11:805–12.
[181] Mège R-M, Gavard J, Lambert M. Regulation of cell–cell junctions by the cytoskeleton. Curr Opin Cell Biol 2006;18:541–8.
[182] Martin AC, Kaschube M, Wieschaus EF. Pulsed contractions of an actin-myosin network drive apical constriction. Nature 2009;457:495–9.
[183] Dawes-Hoang RE, Parmar KM, Christiansen AE, Phelps CB, Brand AH, Wieschaus EF. Folded gastrulation, cell shape change and the control of myosin localization. Development 2005;132:4165–78.
[184] Ganz A, Lambert M, Saez A, Silberzan P, Buguin A, Mège R-M, et al. Traction forces exerted through N-cadherin contacts. Biol Cell 2006;98:721–30.
[185] Liu Z, Tan JL, Cohen DM, Yang MT, Sniadecki NJ, Ruiz SA, et al. Mechanical tugging force regulates the size of cell–cell junctions. Proc Natl Acad Sci U S A 2010;107:9944–9.
[186] Sniadecki NJ, Lamb CM, Liu Y, Chen CS, Reich DH. Magnetic microposts for mechanical stimulation of biological cells: fabrication, characterization, and analysis. Rev Sci Instrum 2008;79:044302–8.
[187] le Digabel J, Biais N, Fresnais J, Berret J-F, Hersen P, Ladoux B. Magnetic micropillars as a tool to govern substrate deformations. Lab Chip 2011;11:2630–6.
[188] Sniadecki NJ, Anguelouch A, Yang MT, Lamb CM, Liu Z, Kirschner SB, et al. Magnetic microposts as an approach to apply forces to living cells. Proc Natl Acad Sci U S A 2007;104:14553–8.
[189] Liang XM, Han SJ, Reems J-A, Gao D, Sniadecki NJ. Platelet retraction force measurements using flexible post force sensors. Lab Chip 2010;10:991–8.
[190] Liu Z, Sniadecki N, Chen C. Mechanical forces in endothelial cells during firm adhesion and early transmigration of human monocytes. Cell Mol Bioeng 2010;3:50–9.
[191] Saez A, Anon E, Ghibaudo M, du Roure O, Di Meglio J-M, Hersen P, et al. Traction forces exerted by epithelial cell sheets. J Phys Condens Matter 2010;22:194119.
[192] Nadarajah B, Alifragis P, Wong ROL, Parnavelas JG. Ventricle-directed migration in the developing cerebral cortex. Nat Neurosci 2002;5:218–24.
[193] Malatesta P, Appolloni I, Calzolari F. Radial glia and neural stem cells. Cell Tissue Res 2008;331:165–78.
[194] Gumera C, Rauck B, Wang Y. Materials for central nervous system regeneration: bioactive cues. J Mater Chem 2011;21:7033–51.
[195] Yao L, Wang S, Cui W, Sherlock R, O'Connell C, Damodaran G, et al. Effect of functionalized micropatterned PLGA on guided neurite growth. Acta Biomater 2009;5:580–8.
[196] Miller C, Jeftinija S, Mallapragada S. Synergistic effects of physical and chemical guidance cues on neurite alignment and outgrowth on biodegradable polymer substrates. Tissue Eng 2002;8:367–78.
[197] Li N, Folch A. Integration of topographical and biochemical cues by axons during growth on microfabricated 3-D substrates. Exp Cell Res 2005;311:307–16.
[198] Mahoney MJ, Chen RR, Tan J, Mark Saltzman W. The influence of microchannels on neurite growth and architecture. Biomaterials 2005;26:771–8.
[199] Gomez N, Lu Y, Chen S, Schmidt CE. Immobilized nerve growth factor and microtopography have distinct effects on polarization versus axon elongation in hippocampal cells in culture. Biomaterials 2007;28:271–84.
[200] Kang E, Jeong GS, Choi YY, Lee KH, Khademhosseini A, Lee S-H. Digitally tunable physicochemical coding of material composition and topography in continuous microfibres. Nat Mater 2011;10:877–83.
[201] Houchin-Ray T, Swift LA, Jang J-H, Shea LD. Patterned PLG substrates for localized DNA delivery and directed neurite extension. Biomaterials 2007;28:2603–11.
[202] Recknor JB, Sakaguchi DS, Mallapragada SK. Directed growth and selective differentiation of neural progenitor cells on micropatterned polymer substrates. Biomaterials 2006;27:4098–108.
[203] Lietz M, Dreesmann L, Hoss M, Oberhoffner S, Schlosshauer B. Neuro tissue engineering of glial nerve guides and the impact of different cell types. Biomaterials 2006;27:1425–36.
[204] Wang M, Zhai P, Chen X, Schreyer DJ, Sun X, Cui F. Bioengineered scaffolds for spinal cord repair. Tissue Eng Part B Rev 2011;17:177–94.
[205] Orive G, Anitua E, Pedraz JL, Emerich DF. Biomaterials for promoting brain protection, repair and regeneration. Nat Rev Neurosci 2009;10:682–92.
[206] Thuret S, Moon LDF, Gage FH. Therapeutic interventions after spinal cord injury. Nat Rev Neurosci 2006;7:628–43.

[207] Wong DY, Leveque J-C, Brumblay H, Krebsbach PH, Hollister SJ, LaMarca F. Macro-architectures in spinal cord scaffold implants influence regeneration. J Neurotrauma 2008;25:1027–37.
[208] He L, Zhang Y, Zeng C, Ngiam M, Liao S, Quan D, et al. Manufacture of PLGA multiple-channel conduits with precise hierarchical pore architectures and in *vitro*/*vivo* evaluation for spinal cord injury. Tissue Eng Part C Methods 2009;15:243–55.
[209] Krych AJ, Rooney GE, Chen B, Schermerhorn TC, Ameenuddin S, Gross L, et al. Relationship between scaffold channel diameter and number of regenerating axons in the transected rat spinal cord. Acta Biomater 2009;5:2551–9.
[210] Rutkowski GE, Miller CA, Jeftinija S, Mallapragada SK. Synergistic effects of micropatterned biodegradable conduits and Schwann cells on sciatic nerve regeneration. J Neural Eng 2004;1:151–7.
[211] Feinberg AW, Feigel A, Shevkoplyas SS, Sheehy S, Whitesides GM, Parker KK. Muscular thin films for building actuators and powering devices. Science 2007;317:1366–70.
[212] Bursac N, Parker KK, Iravanian S, Tung L. Cardiomyocyte cultures with controlled macroscopic anisotropy: a model for functional electrophysiological studies of cardiac muscle. Circ Res 2002;91:e45–54.
[213] Kajzar A, Cesa CM, Kirchgessner N, Hoffmann B, Merkel R. Toward physiological conditions for cell analyses: forces of heart muscle cells suspended between elastic micropillars. Biophys J 2008;94:1854–66.
[214] Zhang T, Wan LQ, Xiong Z, Marsano A, Maidhof R, Park M, et al. Channelled scaffolds for engineering myocardium with mechanical stimulation. J Tissue Eng Regen Med; 2011. doi:10.1002/term.481.
[215] Heidi Au HT, Cui B, Chu ZE, Veres T, Radisic M. Cell culture chips for simultaneous application of topographical and electrical cues enhance phenotype of cardiomyocytes. Lab Chip 2009;9:564–75.
[216] Yin L, Bien H, Entcheva E. Scaffold topography alters intracellular calcium dynamics in cultured cardiomyocyte networks. Am J Physiol Heart Circ Physiol 2004;287:H1276–85.
[217] Kim J, Park J, Na K, Yang S, Baek J, Yoon E, et al. Quantitative evaluation of cardiomyocyte contractility in a 3D microenvironment. J Biomech 2008;41:2396–401.
[218] Patel AA, Desai TA, Kumar S. Microtopographical assembly of cardiomyocytes. Integr Biol (Camb) 2011;3:1011–9.
[219] Engelmayr Jr GC, Cheng M, Bettinger CJ, Borenstein JT, Langer R, Freed LE. Accordion-like honeycombs for tissue engineering of cardiac anisotropy. Nat Mater 2008;7:1003–10.
[220] Kneser U, Schaefer DJ, Polykandriotis E, Horch RE. Tissue engineering of bone: the reconstructive surgeon's point of view. J Cell Mol Med 2006;10:7–19.
[221] Freed LE, Engelmayr Jr GC, Borenstein JT, Moutos FT, Guilak F. Advanced material strategies for tissue engineering scaffolds. Adv Mater 2009;21:3410–8.
[222] Kenar H, Kocabas A, Aydinli A, Hasirci V. Chemical and topographical modification of PHBV surface to promote osteoblast alignment and confinement. J Biomed Mater Res A 2008;85:1001–10.
[223] Holthaus MG, Stolle J, Treccani L, Rezwan K. Orientation of human osteoblasts on hydroxyapatite-based microchannels. Acta Biomater 2012;8:394–403.
[224] Kirmizidis G, Birch MA. Microfabricated grooved substrates influence cell-cell communication and osteoblast differentiation in vitro. Tissue Eng Part A 2009;15:1427–36.
[225] Kim IL, Mauck RL, Burdick JA. Hydrogel design for cartilage tissue engineering: a case study with hyaluronic acid. Biomaterials 2011;32:8771–82.
[226] Hutmacher DW. Scaffolds in tissue engineering bone and cartilage. Biomaterials 2000;21:2529–43.
[227] Hamilton DW, Riehle MO, Monaghan W, Curtis AS. Chondrocyte aggregation on micrometric surface topography: a time-lapse study. Tissue Eng 2006;12:189–99.
[228] Moutos FT, Freed LE, Guilak F. A biomimetic three-dimensional woven composite scaffold for functional tissue engineering of cartilage. Nat Mater 2007;6:162–7.
[229] Narang D, Sood S, Thomas MK, Dinda AK, Maulik SK. Effect of dietary palm olein oil on oxidative stress associated with ischemic-reperfusion injury in isolated rat heart. BMC Pharmacol 2004;4:29.
[230] Hakem R, de la Pompa JL, Sirard C, Mo R, Woo M, Hakem A, et al. The tumor suppressor gene Brca1 is required for embryonic cellular proliferation in the mouse. Cell 1996;85:1009–23.
[231] Choi YY, Chung BG, Lee DH, Khademhosseini A, Kim JH, Lee SH. Controlled-size embryoid body formation in concave microwell arrays. Biomaterials 2010;31:4296–303.
[232] Marty R, Fuentes C. Aspects tridimensionnels du cortex cérébral: Étude par la méthode de Golgi-Cox souséclairage incident. Brain Res 1968;11:124–33.
[233] Gros T, Sakamoto JS, Blesch A, Havton LA, Tuszynski MH. Regeneration of long-tract axons through sites of spinal cord injury using templated agarose scaffolds. Biomaterials 2010;31:6719–29.